

THE EXTREMES OF CONTINUUM AND EMISSION-LINE VARIABILITY OF AGN: CHANGING-LOOK EVENTS AND BINARY SMBHS

S. Komossa¹  and D. Grupe² 

¹*Max-Planck-Institut für Radioastronomie, Auf dem Hügel 69, 53121 Bonn, Germany*
E-mail: skomossa@mpifr.de

²*Department of Physics, Geology, and Engineering Technology, Northern Kentucky University,
1 Nunn Drive, Highland Heights, KY 41099, USA*

(Received: November 11, 2024; Accepted: November 11, 2024)

SUMMARY: The extremes of emission-line and continuum variability of Active Galactic Nuclei (AGN) are unique probes of the physics and geometry of the central engine. This review provides an overview of the most extreme cases of continuum and optical emission-line variability of AGN and the proposed interpretations. We also point out remaining challenges in the identification of changing-look (CL) AGN and discuss future prospects. This includes the need for identification of larger samples of CL narrow-line Seyfert 1 galaxies and CL LINERs at opposite ends of the accretion regime. In the second part, evidence for semi-periodic variability of broad lines and continuum emission, and its possible interpretation by the presence of binary SMBHs is addressed. Most recent results from the project MOMO are presented which monitors densely the best-known binary SMBH candidate OJ 287. In the last few years, the results from this project have ruled out the leading binary model and clearly established the need for new binary modeling in an entirely different parameter regime and based on the actually measured (primary) SMBH mass of $10^8 M_{\odot}$. Ongoing and near-future time-domain surveys, and first gravitational wave detections of single systems, will play an important role in advancing this frontier in astrophysics.

Key words. Galaxies: nuclei – Galaxies: Seyfert – quasars: emission lines – quasars: supermassive binary black holes – accretion disks

1. INTRODUCTION

Active Galactic Nuclei (AGN) are the most luminous long-lived, compact objects in the universe. Their luminous radiation across the electromagnetic spectrum is thought to be the result of accretion of matter onto the supermassive black hole (SMBH) at their center; an idea which emerged in the 1960s (Salpeter 1964, Lynden-Bell 1969). Ever since their discovery (Seyfert 1943) variability has played a major role in the study and interpretation of AGN (Ul-

rich et al. 1997). For instance, the rapid variability especially discovered in X-rays was used as one of the key arguments that AGN are powered by SMBHs. The rapidity of variability implies a very small dimension of the emission region of just a few gravitational radii $r_g = GM/c^2$ from which the large luminosity arises. A few percent of all massive galaxies host AGN. SMBHs are thought to reside at the centers of many or most galaxies, but are dormant most of the time, not actively accreting significant amounts of matter from their environment and thus not observable as AGN. Such SMBHs are detected by other means (see Graham 2016, for a detailed review).

The SMBH–accretion-disk region is surrounded by two line emitting regions, the broad-line region (BLR) which likely forms part of the outer accretion

© 2024 The Author(s). Published by Astronomical Observatory of Belgrade and Faculty of Mathematics, University of Belgrade. This open access article is distributed under CC BY-NC-ND 4.0 International licence.

disk, and the narrow-line region (NLR) which consists of ISM clumps in the host galaxy. Both these regions are photoionized by the broad-band continuum emission from the accretion disk. While the BLR, of high gas density and small separation from the nucleus (light-days to light-months), responds rapidly to changes in the photoionizing continuum emission, the NLR of lower density and larger distances from the nucleus (parsecs to kiloparsecs) reflects an average of the reprocessed continuum luminosity and variability over thousands of years. Based on the relative strengths and prominence of the broad Balmer lines $H\alpha$ and $H\beta$, AGN are classified into type 1 (dominance of broad lines) and type 2 (absence of broad lines), and several subtypes inbetween (Osterbrock 1989).

Even though in the vast majority of AGN the BLR cannot be spatially resolved with current techniques, its size can be measured indirectly from the time lag between changes in the photoionizing continuum itself and the subsequent BLR emission-line response (Blandford and McKee 1982, Gaskell and Sparke 1986). The technique of BLR reverberation mapping has developed into the most important method of measuring the masses of SMBHs in AGN (Netzer and Peterson 1997), the majority of them ranging between 10^6 and $10^9 M_{\odot}$.

Further, time delays between the X-ray emission produced in the immediate vicinity of the SMBH in or near the inner accretion disk, and the longer-wavelength UV-optical emission thought to arise at least partly from reprocessing further out in the accretion disk, have enabled (order-of-magnitude) estimates of the sizes of the accretion disks around the SMBHs (Edelson et al. 2019).

A fraction of all AGN launches powerful jets often extending beyond the confines of the optical host galaxy up to kpc or Mpc scales. Their radio emission is powered by synchrotron emission of relativistic electrons accelerated in magnetic fields (Urry 1998). If directed at the observer, beaming enhances any variability intrinsic to the jet, and blazars are therefore known to be highly variable. Most of this review rather focuses on intrinsic variability of radio-quiet AGN.

While many AGN are known to be variable by a factor of a few, giant-amplitude variability exceeding factors of 70–100 is rare among AGN in X-rays and even more so in the optical regime. It is these extreme kinds of variability – either in amplitude in form of outbursts or deep low-states, or changing looks, and/or exceptional spectral states, – which are the focus of this review.¹ In addition, in the second

¹The highest amplitudes of X-ray variability recorded to date from the cores of galaxies, exceeding factors of 1000, have been nearly exclusively observed in *non-active* galaxies in the form of temporary flares from stars tidally disrupted by dormant SMBHs (stellar tidal disruption events; TDEs). TDEs will not be discussed much further here (see Komossa 2015, for a review).

part, we address the topic of semi-periodic variability and the search for SMBH binaries in AGN.

High-amplitude variability of AGN was noticed early in individual AGN in the optical band. It was the large-area or all-sky surveys which then played an important role in identifying extreme cases of AGN variability and put results on a statistical basis, for instance in X-rays in the course of early all-sky surveys with Uhuru (Forman et al. 1978) and ROSAT (Truemper 1982), or in the optical band with photographic plates² and the Sloan Digital Sky Survey (SDSS; York et al. 2000).

SMBHs in AGN and their immediate environment are powerful probes of the physics of matter under extreme conditions: strong gravitational fields and relativistic velocities where special and general relativistic effects prevail, highest gas densities, strongest magnetic fields, and densest radiation fields. The extremes of variability among AGN provide us with valuable insights into the underlying drivers and physics of the central engine. In the X-ray regime, extreme flux and spectral states can reveal the nature of the inner accretion disk, probe the physics of matter under strong gravity, may allow us to measure SMBH spins, and they can uncover the mechanisms responsible for the ejection of matter from the SMBH in form of strong outflows. In the optical regime, AGN with highly variable emission lines provide us with important new constraints on the physics and geometry of the outer accretion disk, the BLR, and the coronal-line region (CLR).

This review is structured as follows: first, we define and discuss optical changing-look AGN (Section 2), their early detections, recent results, a classification scheme, their frequency based on larger surveys, and events in special sub-groups of AGN (Narrow-line Seyfert 1 galaxies and LINERs). In Section 3, we review the properties of individual AGN which stand out by their extreme continuum and/or emission-line variability. Section 4 provides an overview over the different types of theoretical models which have been proposed to explain the high-amplitude variability of AGN, followed by Section 5 on the non-AGN-related mechanisms of high-amplitude continuum and emission-line variability that could mimic the presence of a CL event. In Section 6 we discuss (semi-)periodic variability of the AGN continuum and/or broad lines and its interpretation in terms of binary SMBHs. Section 7 addresses the future prospects and identifies a number of important steps forward, and Section 8 provides a summary and conclusions. Throughout this review, we use a cosmology with $H_0=70 \text{ km s}^{-1} \text{ Mpc}^{-1}$, $\Omega_M=0.3$, and $\Omega_\Lambda=0.7$, and the cosmology calculator of Wright (2006).

²<https://doi.org/10.26131/IRSA441>
<https://www.ipac.caltech.edu/doi/10.26131/IRSA441>

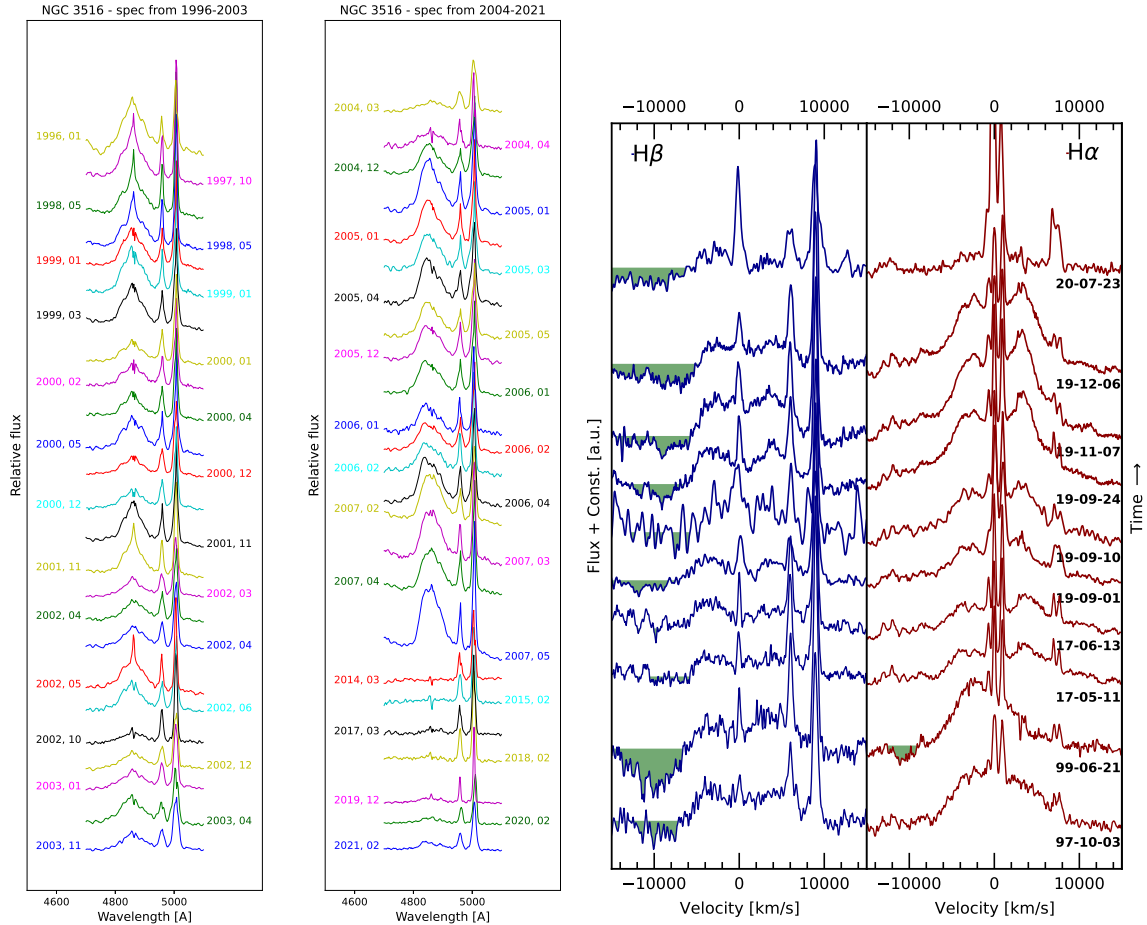


Fig. 1: Examples of optical spectra of changing-look AGN. **Left:** NGC 3516 keeps changing its Seyfert-type between type 1 and type 1.9 showing highly variable Balmer emission lines. The line profile of H β (and the neighbouring [OIII] emission) is shown between the years 1996 and 2021. Adopted from Popović et al. (2023). **Right:** IRAS 23226-3843 showed remarkable changes in its Balmer-line profile, varying between Seyfert type 1 with double- or single-peaked broad Balmer lines between 1997 and 2019. In 2020, the Balmer lines had nearly disappeared, corresponding to a type 1.8 state. The line profiles of H β and H α are shown in velocity space after subtraction of the spectrum of the host galaxy. Adopted from Kollatschny et al. (2023).

2. CHANGING-LOOK AGN

2.1. Definition and early observations

The term changing-look (CL) AGN was initially coined to describe AGN with X-ray spectra that transition between mildly absorbed (Compton-thin) and heavily absorbed (Compton-thick) states (Matt et al. 2003). These systems continue to provide us with important insights into the geometry and kinematics of absorbing material in the central region of AGN. If the absorbing material is located only along our line-of-sight and/or dust-free, the optical emission lines remain mostly unaffected. However, in recent years, the term changing-look has been widely used to refer to optical spectroscopic variability which temporarily or permanently (the latter more rare) changes the classification of the AGN type (e.g. LaMassa et al.

2015), from type 1 (presence of strong broad Balmer lines which dominate over the narrow lines) into types 1.8, 1.9, or 2 (faintness or absence of broad Balmer lines), and vice versa. We use the latter definition throughout this review.

Individual CL AGN were noticed already decades ago (e.g. Andriolat and Souffrin 1968, Tohline and Osterbrock 1976, Alloin et al. 1985, Kollatschny and Fricke 1985, Cohen et al. 1986), the majority of them identified serendipitously when repeated optical spectroscopy was performed on timescales of months to years. Early interpretations included changes in the ionizing continuum or cloud motions. A prominent example is the nearby AGN NGC 4151. It is one of the intermediate-type Seyfert galaxies in the sample of Seyfert (1943). After early evidence for strong Balmer-line variability (Anderson

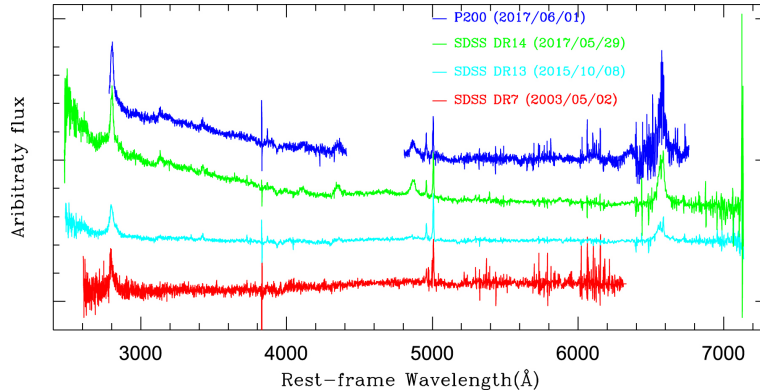


Fig. 2: Example of optical broad-band spectra of the changing-look quasar SBS 1411+533 identified from SDSS between 2003 and 2017. The two strongest emission lines are MgII at the short wavelength end and H α at the long wavelength end. All spectra were transformed to the rest frame, and shifted vertically by an arbitrary amount. Adopted from Wang et al. (2018).

and Kraft 1969), the broad Balmer lines of NGC 4151 decreased strongly in 1984 (Penston and Perez 1984, Lyutyj et al. 1984). They were hardly detected any longer (Penston and Perez 1984, Kielkopf et al. 1985), but had already reverted back to their normal emission levels in January 1985 (Peterson 1985). Fig. 1 displays two examples of CL AGN optical spectra, identified in the course of reverberation mapping and long-term spectroscopy over decades [NGC 3516; Popović et al. (2023)] or triggered as follow-ups of high-amplitude continuum variability [IRAS 23226-3843; identified after a strong decline of the X-ray continuum emission in the XMM-Newton slew survey (Kollatschny et al. 2023)]. The optical spectra which let to the identification of a changing-look quasar are shown in Fig. 2, based on SDSS and follow-up optical spectroscopy (Wang et al. 2018).

2.2. Recent developments

The topic of CL AGN received great attention during the last decade for several different reasons: larger samples of CL AGN were identified from optical surveys, more extreme cases were discovered, events were found not only in Seyfert galaxies but also in luminous quasars where the emitting regions are much more extended so that longer variability timescales are generally expected, and exceptionally high amplitudes of variability were detected not only in X-rays that are thought to arise in or near the innermost accretion disk, but in the optical emission as well, arising from more extended spatial scales where rapid and high-amplitude variability is less expected. The rapid and high-amplitude changes especially in the high-luminosity quasars pose challenges to accretion-disk models, and have triggered the development of many new ideas, and new scenarios to explain fast disk changes have been explored in recent years (Section 4).

Well studied single AGN with densely covered light curves and/or spectra have showcased the exceptional variability properties and have placed tight constraints on disk models. A dense 70 day monitoring campaign from the NIR to X-rays of high-amplitude continuum and line variability of NGC 2617 allowed to establish the X-ray emission as driver of the NIR-UV emission in this system (Shappee et al. 2014). Mrk 590 was found to fade dramatically in the optical continuum emission by a factor 100 over a period of decades. Once a classical type 1 AGN, only faint the broad H α emission remained in its lowest state in 2012 (Denney et al. 2014). Since then, it partially re-ignited and went into a state of repeat flaring activity, with a strong correlation between the X-ray and UV emission, and a characteristic UV variability timescale of 100 days (Lawther et al. 2023). The CL event of 1ES1927+654 was initially discovered as an optical transient and is characterized by rapid and high-amplitude variability that is decoupled between the optical and X-rays (Trakhtenbrot et al. 2019, Ricci et al. 2020). Delayed radio jet formation was detected (Meyer et al. 2024). NGC 1566 is remarkable for changing its Seyfert type multiple times since the 1980s (Alloin et al. 1985, Ochmann et al. 2024). The Seyfert 1 galaxy IRAS 23226-3843 is characterized by extremely broad and often double-peaked broad Balmer lines which nearly disappeared in its type 1.9 state (Kollatschny et al. 2020), discovered after a factor 30 drop in X-rays. The Seyfert 1.9 galaxy IC 3599 stands out due to its exceptionally high-amplitude continuum variability in the X-rays and EUV accompanied by a strong emission-line response including high-ionization lines identified early in the 1990s (Section 5). The first CL event discovered in a high-luminosity system, i.e. in a quasar, SDSS J015957.64+003310.5, (LaMassa et al. 2015) transitioned between type 1 and 1.9 within 10 years. At even higher redshift, the quasar

SDSS J141324.27+530527.0 changed from type 1.9 to type 1 within ~ 10 years (Wang et al. 2018).

Overall, the CL events show a rich phenomenology, with fast and slow events which ultimately revert back to their original states, nearly full turn-on and turn-off events, and events which repeat; all of these within timescales of months to years. Full turn-offs are rare. In many cases, a faint broad component in H α is still detected in sensitive low-state spectra (e.g. Denney et al. 2014, McElroy et al. 2016, Parker et al. 2016, Kollatschny et al. 2023, Temple et al. 2023, Popović et al. 2023). Even if the direct components of BLR and continuum disappeared, as long as a few percent of them are seen in scattered light, these components would only fade at much longer timescales (Hutsemékers et al. 2019).

Komossa et al. (2024) suggested the following classification (Table 1) of CL events (not yet based on physical models, because too many different mechanisms of accretion-disk variability have been suggested in the last few years and it is not yet clear which mechanisms dominate, and several different ones likely come with similar observational properties): Type I CL events show a slow turn-on in continuum and broad emission lines on a timescale of years to decades. Type II events show a turn-off on the same timescales. Type III CL AGN display fast transient outburst events with rise times of weeks to months, and type IV events show rapid dimmings on similar timescales. Type V events are characterized by more regular and recurrent brightenings and fades; a behaviour shown by many AGN which are selected for reverberation mapping. Finally, the category VI events exhibit a frozen look (Komossa et al. 2020a) meaning that the broad emission lines do not respond to changes in the observed continuum emission. Events in all categories may repeat, even though the number of recurrent CL AGN so far identified is still small (Wang et al. 2024a,b).

2.3. Frequency of CL AGN

Different approaches have been used to detect the CL events, either based on identification of high-amplitude continuum flux changes in the optical, IR or X-rays first (in individual objects or dedicated searches in ongoing or archival large surveys) then followed by spectroscopic follow-ups, or based on spectroscopic searches including regular reverberation mapping of AGN.

Spectroscopic surveys covering large areas of the sky represent excellent data bases for selecting samples of CL AGN. Ultimately, these will provide us with the frequency, variability timescales, and accretion disk and host galaxy properties of CL events at all luminosities. Systematic searches for CL AGN have been performed on the optical data bases of, e.g. LAMOST (Yang et al. 2018), 6dFGS/SkyMapper (Hon et al. 2022), and DESI (Guo et al. 2024), or in the WISE mid-infrared regime, the latter with focus

on the IR continuum variability, and ongoing follow-ups to distinguish between TDEs and AGN (Jiang et al. 2021). Primarily, the rich SDSS database (York et al. 2000) has been extensively used to select larger samples of AGN with multiple spectroscopic observations within SDSS, or were observed once with SDSS and then followed-up at other telescopes (e.g. Runco et al. 2016, Ruan et al. 2016, MacLeod et al. 2016, 2019, Graham et al. 2020, Potts and Villforth 2021, Green et al. 2022, Zeltyn et al. 2024, Dong et al. 2024). These searches have started to quantify the characteristics and frequency of the different categories of CL events in Seyfert galaxies and quasars.

Runco et al. (2016) evaluated the frequency of CL events in nearby Seyfert galaxies. Their initial sample consists of Seyfert 1 galaxies selected from SDSS, then followed up with renewed spectroscopy at the Keck telescope. They reported an occurrence of 10% CL events in this Seyfert sample. The occurrence rate of CL quasars was found to be much lower. MacLeod et al. (2016) reported a fraction of $\sim 1\%$ CL events in their sample of SDSS quasars. An approximately equal number of events evolved toward the type 1 state, or toward the type 2 state. The most recent sample of CL AGN selected from SDSS V (Zeltyn et al. 2024) comprises 33% CL events that showed brightening, and 67% that showed dimming. In that sample, the CL AGN have a median accretion rate of $L/L_{\text{Edd}} = 0.025$, slightly lower than in a control sample with $L/L_{\text{Edd}} = 0.043$.

Archival searches on large spectroscopic samples are well suited for statistical inferences on the CL AGN population as a whole. An alternative approach has concentrated on rapid identification of new CL events while they happen (for instance, with Swift, the XMM-Newton slew survey, GAIA, or ASAS-SN) followed up rapidly by multiwavelength observations within days to weeks (e.g. Parker et al. 2016). That way, dense monitoring of the ongoing, evolving event at multiple wavelengths is possible. Representatives of such AGN are discussed in Section 5.

2.4. Selection effects and other considerations

It has to be kept in mind, that so far the selection criteria used to identify CL AGN (e.g. the required amplitude of flux variability in the BLR emission and/or the continuum, or the required Seyfert-type change for instance from type 1 into 1.9, or only from type 1.5 into 1.8) have varied between different studies. This fact has to be taken into account when direct comparisons between different surveys and samples are made.

Other selection effects operate as well: For instance, if the initial parent sample comprises mostly or entirely type 1 AGN, then turn-off events (i.e., a dimming in line and continuum brightness) will be preferentially identified in any later follow-up observations. If instead the parent sample consists only

Table 1: CL AGN classification scheme proposed by Komossa et al. (2024) based on the different types and timescales of continuum variability and emission-line response. All categories may repeat.

category	CL classification	timescale
I	slow turn-on	years–decades
II	slow turn-off	years–decades
III	rapid transient event: outburst	rise time: weeks to months
IV	rapid transient event: deep drop	fade time: weeks to months
V	regular brightenings and fades	weeks to years
VI	frozen-look events	any time

of type 2 AGN, then only turn-ons, if any, will be found at the second epoch of spectroscopy. Further, the amplitude of the type change (from type 1 or 1.5 into type 1.8, 1.9, or 2) will show a strong dependency on telescope sensitivity, since faint broad Balmer lines are more difficult to identify in spectra of lower signal-to-noise ratio.

Further, and this effect is important, AGN with already faint Balmer lines (lower Eddington accretion rates at fixed SMBH mass) will be preferentially detected as CL AGN, because only a small luminosity change is required to make the broad lines undetectable and, therefore, make the AGN appear as CL. This effect will cause an apparent trend towards lower Eddington accretion-rate AGN showing CL events more often. Instead, when the broad lines are luminous, a much larger actual change in luminosity is required to identify the CL event in the first place. An alternative approach could therefore be to introduce the requirement of a fixed minimum factor (10) of variability, independent of the exact AGN type, to search for CL AGN, even though this would not include events in faint systems where a small decrease of brightness already makes the continuum and BLR undetectable.

Finally, it has to be kept in mind, that there is one instrumental effect, which can cause spurious CL events. This happens when the slit or fiber is not placed on the very nucleus of the galaxy, as it can happen preferentially for the nearby galaxies widely extended in the sky. If the slit or fiber misses the very nucleus, the pointlike BLR and continuum emission will appear faint or absent (depending on the value of the atmospheric seeing and the slit width), while the extended NLR will still be detected. Such spectra will mimic CL events even if the emission is intrinsically constant.

2.5. CL events across the quasar main sequence

It is interesting to ask, how CL AGN change across the quasar main sequence. The AGN emission-line properties have been used to evaluate differences across the whole AGN population using principal component analyses (e.g. Boroson and Green 1992, Sulentic et al. 2000, Grupe 2004, Xu et al. 2007,

Marziani et al. 2018). The AGN main sequence, the distribution of AGN in a diagram which plots the FWHM of the broad Balmer line, $\text{FWHM}(\text{H}\beta)$, against the strength of the FeII emission, R_{FeII} (defined as the flux ratio of $\text{FeII} 4570/\text{H}\beta$, where $\text{FeII} 4570$ is integrated between 4434 and 4684Å) has been established as a powerful tool to uncover the physical parameters which drive the properties of AGN, and two main populations, A and B, are distinguished. The accretion rate has been found to be the main driver across the diagram, inclination playing a secondary role (see Marziani et al. 2018, for a review). The variation of CL events across the quasar main sequence only starts to be explored. Panda and Śniegowska (2024) found that the majority of the CL AGN of their sample does not cross between populations A and B, but remains within population B during the whole CL event. Only 5 out of their 32 sources change between population A and B, and during this process none of them develops into the Narrow-line Seyfert 1 regime where $\text{FWHM}(\text{H}\beta) < 2000 \text{ km/s}$.

2.6. CL events in NLS1 galaxies

The majority of CL events have so far been observed in broad-line Seyfert 1 (BLS1) galaxies. Narrow-line Seyfert 1 (NLS1) galaxies are defined as a subgroup of AGN with particular emission-line properties (Goodrich 1989) which place them at one extreme end of AGN correlation space (Sulentic et al. 2000, Boroson 2002, Grupe 2004, Xu et al. 2012). Their properties are driven by their low-mass SMBHs accreting preferentially near the Eddington limit and, as such, NLS1s are of special interest also as local counterparts to rapidly growing SMBHs at high redshift at the epoch of galaxy formation. Further, as near-Eddington accretors they allow to test disk-variability/instability scenarios which operate at these rates (Section 4). Plus, many NLS1 galaxies are known to be highly variable in X-rays, and for all these reasons the question is raised of how many NLS1s undergo CL events. Up to now, many dedicated large-sample searches rather focussed on BLS1 galaxies (i.e., involving an $\text{FWHM}(\text{H}\beta) > 2000 \text{ km/s}$ cut-off criterion, excluding NLS1s).

So far, only a few CL events in candidate NLS1 galaxies have been identified, summarized in Ta-

Table 2: Summary of the CL events so far identified in candidate NLS1 galaxies. Column (1): galaxy name, (2): redshift z , (3): FWHM of broad $H\beta$, and (4): observed variability timescale Δt of the spectroscopic type change. Since often only two spectra were taken years apart, it is well possible, and even likely, that the actual variability timescale is much shorter and/or that the AGN changed its type multiple times in between. Δt can therefore be regarded as the upper limit. NGC 1566 changed within months from one type to the other and, in this case, we list Δt of the fastest recorded type change. Column (5): lists reference(s) for the identification of the CL event and/or the FWHM measurement ([1]=Brandt et al. (1995), [2]=Grupe et al. (1995b), [3]=Komossa and Bade (1999), [4]=MacLeod et al. (2019), [5]=Liu et al. (2019), [6]=Frederick et al. (2019), [7]=Hon et al. (2022), and [8]=Alloin et al. (1985)). Column (6) provides comments.

name	z	FWHM($H\beta$) km/s	Δt yrs	ref	comments
(1)	(2)	(3)	(4)	(5)	(6)
NGC 1566	0.005	1950	0.33	[8]	recurrent Seyfert-type changes
IC 3599	0.021	1200	0.75	[1,2,3]	two giant outbursts separated by 20 yrs; no bona-fide NLS1, no FeII
SDSS J123359.12+084211.5	0.256	2430	11	[4,5]	change in both, Balmer lines & FeII
ZTF18aajupnt	0.037	940	16	[6]	spectral change from LINER to NLS1
J1406507-244250	0.046	3000	18	[7]	little optical continuum variability

ble 2.³ Larger samples are expected from SDSS V (Kollmeier et al. 2019) and LSST (Ivezić et al. 2019), for instance, and detailed studies of single systems will be made possible in X-rays with the space mission SVOM (Wei et al. 2016, Xu et al. 2024). Among the five CL galaxies in Table 2, NGC 1566 and IC 3599 stand out due to their well-covered longterm light curves spanning decades, and both of them show unique properties further discussed in Section 5, even though it has to be kept in mind that IC 3599 lacks FeII emission, often included as one of the defining characteristics of NLS1 galaxies (Véron-Cetty et al. 2001).

Identifying NLS1 galaxies in their turn-off states offers a great wealth of new applications w.r.t understanding NLS1 physics, highlighted by Xu et al. (2024). First, CL NLS1 galaxies in their type 2 states will enable us for the first time to study the properties of their circum-nuclear environment (e.g. in form of the X-ray ISM and/or the presence of outflows), since unlike broad-line Seyfert galaxies, there is no immediate way to identify the type 2 counterparts of the NLS1 population (except for spectropolarimetry which has rarely identified candidates so far; Pan et al. 2019). Second, in type 2 states without the bright continuum emission which hampers such studies in the type 1 state, the host galaxies will become more easily detectable, and their properties can be measured. The same holds for stellar velocity dispersion measurements (and therefore SMBH mass estimates), as well as stellar population measurements that would also shed new light on the evolutionary state of the systems. Third, type 2 states will enable

us to study the location of the galaxies in diagnostic diagrams, so far hampered by the challenges of the BLR-NLR line profile decompositions in cases where the FWHM of the broad component itself is rather small. Finally, comparisons between the CL BLS1 and CL NLS1 galaxies will highlight differences in their accretion disk properties and, especially, will allow us to address the question, whether different accretion disk instabilities and/or other disk variability mechanisms are operating at different Eddington ratios.

2.7. CL events in LINERs

Low-ionization nuclear emission regions (LINERs) are defined by their location in emission-line diagnostic diagrams of galaxies (Osterbrock 1989), and represent a mixed class of objects. Some are powered by AGN, as evidenced by the presence of broad Balmer lines in their optical spectra, others are excited by stars, and LINER-like emission-line ratios can also arise through shocks, or by other processes in the ISM of elliptical galaxies, or even the intracluster gas.

During the first months of operation of the Zwicky Transient factory (ZTF), five galaxies with LINER-like spectra in quiescence that show only narrow emission lines in low-state, were detected as new transients. Follow-up optical spectroscopy revealed their transformation into broad-line AGN (Frederick et al. 2019).⁴ Among these changing-look LINERs, one system transformed into an NLS1 optical spectrum (see Section 2.6, and Table 2). This new class of

³See Section 3 for the case of PS16dtm (SN 2016ezh). The nature of this event has not yet been identified with certainty and it may rather represent a supernova or TDE than a NLS1 galaxy.

⁴A few other LINERs with transient continuum emission or enhanced UV emission have been identified in the past. However, some of these events could have been TDEs. The most reliable CL AGN events in LINERs would be long-lived switch-ons (see also Section 3).

changing-look LINERs provides us with important new constraints on the accretion state in LINER galaxies.

2.8. CL events in blazars

A small number of blazars show high-amplitude variability in (some of) their broad emission lines. It is well possible, that some of these still represent a response to changes in the accretion-disk luminosity. However, other recorded incidences of blazar broad-line variability were peculiar, and affected only certain emission lines (see, e.g. the MgII variability event of CTA 102; [Chavushyan et al. 2020](#)) and these events are likely related to individual jet-cloud interactions, and excited by the local non-thermal continuum emission from the jet. These are therefore due to a different and jet-related mechanism, and we do not discuss the CL blazars any further here (see [Foschini et al. 2021](#), for defining CL blazars as AGN that change between FSRQ and BL Lac classification).

3. MIMICRY

Not all broad-line variability in galaxies is caused by the CL phenomenon in AGN. There is some mimicry from unrelated processes, especially from (1) the disruption and accretion of single stars in quiescent galaxies or in AGN (tidal disruption events; TDEs), and from (2) the explosions of supernovae of type II_n. Both types of events can come with temporary broad and/or narrow optical emission lines which look temporarily similar to the lines in AGN and would thus mimic CL AGN.

When TDEs were first discovered, it was important to identify them in *quiescent* host galaxies, to be sure we saw TDEs and not just accretion-disk processes in long-lived AGN ([Rees 1990](#), [Komossa and Bade 1999](#)). Further, it was initially assumed that TDEs were single events not repeating on timescales of years given the TDE rate of $\sim 10^{-4}$ events per galaxy per year ([Stone and Metzger 2016](#)), and detection of repeat flaring on that timescale was therefore initially thought to falsify any TDE interpretation. Meanwhile, it has been shown that TDEs may appear as double outbursts if the affected stars are in a binary system ([Mandel and Levin 2015](#)). Further, partial tidal stripping events of orbiting stars can cause repeat flaring ([MacLeod et al. 2013](#)), and if tidal disruption occurs in binary SMBH systems, phases of interrupted and re-started accretion episodes imply a highly variable light curve as well ([Liu et al. 2014](#)). Therefore, light curves of such TDEs may also appear similar to accretion-disk instability powered light curves in AGN, making the distinction of the processes *in AGN* more challenging, especially in cases of only short-time light curve coverage. Meanwhile, cases of recurrent TDEs in *quiescent* host galaxies have been reported (e.g. [Malyali et al. 2023](#)). On the other hand, supernovae of type

II_n, even though very similar to CL AGN in their optical spectra, can be distinguished by their faint or absent X-ray emission. Yet, there is a number of transients, which so far elucidated a unique classification ([Wiseman et al. 2024](#)). PS16dtm (SN 2016ezh) is a good example. It shows properties of all three phenomena, a TDE, superluminous SN, and CL NLS1, and all three interpretations have been proposed and discussed in the literature ([Terreran et al. 2016](#), [Dong et al. 2016](#), [Blanchard et al. 2017](#), [Petrushevska et al. 2023](#)).

In any case, TDEs are very rare events, therefore in a statistical sense we can be certain that at most a small fraction of CL AGN could be mimicked by TDEs, because the observed frequency of CL events in nearby galaxies ([Runco et al. 2016](#)) is far too high.

We do not discuss TDEs and SNe any further here (see [Komossa and Bade 1999](#), [Komossa et al. 2009](#), for a detailed discussion of these events, and how to further distinguish them from the AGN-related variability processes).

Finally, as opposed to changes in a long-lived accretion disk in an AGN, temporary events powered by the accretion of an ISM clump can cause a short-lived CL-AGN-like phenomenon ([Wiseman et al. 2023](#)), if the environment itself is gas rich, such that broad lines may appear for a short time. These events differ from the long-lived AGN in their absence or faintness of the NLR emission.

4. THEORETICAL MECHANISMS OF HIGH-AMPLITUDE AGN VARIABILITY

Recent CL AGN results, especially the events in high-luminosity AGN (quasars) and at highest amplitudes and/or shortest timescales of variability have motivated many new theoretical studies of disk-variability mechanisms, adding to the decades-old disk-instability models (e.g. [Lightman and Eardley 1974](#)).

High-amplitude variability can be explained by two fundamentally different mechanisms. The first one is intrinsic variability where the emission of the accretion disk and BLR itself changes. The second is apparent variability caused by the effects of gas absorption and dust extinction, or by the effect of gravitational lensing, acting on the intrinsically constant emission regions. We briefly review the different models and processes in turn, the intrinsic mechanisms first.

4.1. Intrinsic variability

The fastest, highest-amplitude events in the luminous systems challenge our understanding of accretion physics, as typical disk variability timescales are long (see compilation by [Stern et al. 2018](#), for order-of-magnitude estimates of disk timescales):

The longest timescale is the viscous timescale, given by

$$t_v \sim 400 \text{ years} \left(\frac{h/R}{0.05}\right)^{-2} \left(\frac{\alpha}{0.03}\right)^{-1} \left(\frac{M_{\text{BH}}}{10^8 M_\odot}\right) \left(\frac{R}{150 r_g}\right)^{3/2}. \quad (1)$$

The thermal timescale is given by

$$t_{\text{th}} \sim 1 \text{ year} \left(\frac{\alpha}{0.03}\right)^{-1} \left(\frac{M_{\text{BH}}}{10^8 M_\odot}\right) \left(\frac{R}{150 r_g}\right)^{3/2}. \quad (2)$$

For comparison, the orbital timescale is short and given by

$$t_{\text{orb}} \sim 10 \text{ days} \left(\frac{M_{\text{BH}}}{10^8 M_\odot}\right) \left(\frac{R}{150 r_g}\right)^{3/2}. \quad (3)$$

Here, M_{BH} is the SMBH mass, α is the disk viscosity parameter, h is the disk height, and R the disk radius.

A large number of new theoretical studies in the last few years have explored new mechanisms for accretion disk structural and emission changes. These include modified lampposts, disk instabilities, disk distortions due to local perturbers, disk precession, influence of magnetic fields, effects on BLR or surrounding gas stability, and the presence of binary SMBHs. Some of these studies explored mechanisms of a more rapid transfer of changes across the accretion disk, for instance, involving magnetic fields, but did not yet address the origin of the high-amplitude outburst in the first place; others focussed directly on the outburst mechanism itself; and yet others explored changes in the BLR structure and the feeding mechanism.

First, different types of accretion disk instabilities have been considered to explain the high-amplitude luminosity changes, including the radiation-pressure instability of the inner disk (Lightman and Eardley 1974, Grupe et al. 2015, Sniegowska et al. 2020), a hydrogen ionization instability (Noda and Done 2018), or instabilities in warped disks at large radii (Raj et al. 2021). An instability in the circumnuclear gas supply has been discussed as well (Wang et al. 2024a). Some models were suggested where the BLR clouds themselves are directly affected by an instability (Nicastro 2000); a model initially proposed to explain the absence of a BLR in systems with low accretion rate.

Other approaches involved disk perturbations due to the presence of local perturbers, like a stellar mass black hole. Once it reaches the innermost regions of the accretion disk, its mass can become comparable to, or even dominate, the co-rotating disk mass, and can then have a strong influence on the inner disk (Stern et al. 2018).

Other approaches invoked the presence of binary SMBHs (see also Section 6), either in form of tidal effects on the mini-disks surrounding both SMBHs of a binary system (Wang and Bon 2020), or effects on the accretion disk during the advanced stages of gravitational wave driven inspirals of binary SMBHs (Zrake et al. 2024).

Alternatively, a modified lamppost model has been suggested (Lawrence 2018), assuming that the X-ray emission which arises from the lamppost is not directly reprocessed by the accretion disk, but rather by a system of dense gas clumps above the disk.

Further, the influence of magnetic fields, or a combination of several effects, has been considered in different ways (Ross et al. 2018, Stern et al. 2018, Dexter and Begelman 2019, Scepi et al. 2021, Pan et al. 2021, Laha et al. 2022, Cao et al. 2023). Another approach focused on highly tilted, precessing, warped accretion disks and the effects of two types of shocks which develop under these conditions (Kaaz et al. 2023).

Finally, there are events in AGN related to stars or TDEs in particular, which could directly affect the accretion disk luminosity and/or disk stability in a long-lived AGN, and thus cause a ‘true’ CL AGN event – as opposed to the TDEs themselves creating their own short-lived broad lines in *quiescent* host galaxies (discussed in Section 3). Star-disk interactions of an orbiting star (Syer et al. 1991) or the debris stream of a TDE (Trakhtenbrot et al. 2019) can increase the disk luminosity at the impact point and thus change the BLR flux, and the same holds for a star that opens a gap in the disk or acts as local perturber of the inner disk (Stern et al. 2018).

4.2. Extrinsic variability

4.2.1. Obscuration: dust extinction and gas absorption

Obscuration by dust-free or dusty gas clouds located between the continuum source (and/or BLR) and the observer can significantly dim the intrinsic emission. The X-ray and optical continuum are affected differently in this situation; the X-rays are mostly affected by gas absorption, the optical mostly by dust extinction.

The broad-band X-ray continuum emission is modified by gaseous matter along the line of sight, imprinting hydrogen and metal K-shell absorption. For gas column densities exceeding $\sim 10^{23-24} \text{ cm}^{-2}$, the material becomes finally Compton-thick and no direct X-rays are detected any longer below 10 keV where the majority of X-ray satellites operates. The optical continuum emission is significantly affected if the absorber contains dust. Extinction causes a characteristic reddening of the continuum shape and a deviation of the BLR Balmer decrement from its (case B) recombination value.

The presence of dust extinction and/or gas absorption can be relatively easily identified through their characteristic effects on the optical and X-ray spectra. Partial obscuration from outflowing dusty clouds in the outer BLR can significantly affect the line profile shapes (Gaskell and Harrington 2018), and single CL AGN are known to show the effects of significant extinction (Potts and Villforth 2021). However, variable obscuration has not been favored as the explanation for the majority of CL events, be-

cause the expected BLR reddening was not observed (Alloin et al. 1985), the optical-UV continuum shape was inconsistent with extinction (MacLeod et al. 2016), the associated X-ray absorption was not observed (Parker et al. 2019b), the hard X-ray (Swift BAT) band is little affected by absorption (Temple et al. 2023), the timescale of variability was too fast (LaMassa et al. 2015), and/or the level of polarization was very low (Hutsemékers et al. 2019).

Dust destruction in response to an intrinsic outburst is another possible mechanism (Oknyansky et al. 2018). It would increase the observed *amplitude* of variability, but may only work once, depending on the mechanisms of dust re-formation.

4.2.2. Gravitational lensing

Gravitational lensing or microlensing can magnify, or de-magnify, the accretion disk and/or the BLR emission. Lensing itself is achromatic, but a moving lens which crosses different parts of an extended emission region like the accretion disk and/or BLR will produce chromatic changes and can cause complex line profile shapes and changes. Microlensing modeling has not yet been much applied to broad-line profile variations of changing-look AGN, but has been studied in lensed quasars (Fian et al. 2021, Savić et al. 2024). The required lensing geometry is rare and the phenomenon is therefore not expected to explain the population of the nearby CL AGN as a whole. A lensing interpretation of the most recent transient event in NGC 1566, involving a binary SMBH, was proposed by Kollatschny and Chelouche (2024).

5. CASES OF EXTREME VARIABILITY OF AGN

Here, we highlight individual AGN which showed some of the most extreme variability known to date (excluding TDEs), and their individual interpretation, focussing on systems which have well-covered longterm light curves in the optical, UV, and X-rays.

All data used for the Neil Gehrels Swift observatory light curves (Swift hereafter; Gehrels et al. 2004) and SEDs presented in this Section were (re)analyzed by us, following the standard procedures in the analysis of Swift XRT (Burrows et al. 2005) and UVOT (Roming et al. 2005) data. In addition to the Swift data from our own projects, archival data were added as well. The X-ray count rates were obtained using tools provided by the UK Swift Science Data Centre at the University of Leicester (Evans et al. 2007).

5.1. Changing-look AGN

5.1.1. NGC 1566

The nearby Seyfert galaxy NGC 1566 is remarkable for going through multiple CL events. It was a bright type 1 AGN in the 1960s (Shobbrook 1966) but faded significantly years later. Optical spectra

acquired between 1980 and 1982 revealed its transition to a type 2 state in 1980. After that, it gradually changed back to a type 1. Another CL event was detected in 1985 (Alloin et al. 1985, 1986). Most of the changes happened rapidly within only four months. The BLR Balmer decrement did not change significantly during the CL event (Alloin et al. 1985).

NGC 1566 is a NLS1 galaxy (Xu et al. 2024) at redshift $z = 0.005$. The NLS1 classification is based on the widths of the broad Balmer lines [FWHM($H\beta$) = 1950 km/s and FWHM($H\alpha$) = 1970 km/s (da Silva et al. 2017, Alloin et al. 1985)], a small ratio of $[OIII]\lambda 5007/H\beta_{total} < 3$, and the detection of Fe II emission complexes (Ochmann et al. 2024).

The most recent outburst of NGC 1566 in the year 2018 was initially reported in the hard X-ray band (Ducci et al. 2018). Multiwavelength follow-up observations, triggered rapidly (Parker et al. 2019b, Oknyansky et al. 2019, Ochmann et al. 2020), then revealed a new CL event. During the outburst (Fig. 3), the optical spectrum changed from type 1.8 to type 1 (Fig. 4) accompanied by strong variations in the helium lines and in several high-ionization iron lines (Oknyansky et al. 2019, Ochmann et al. 2024). The FWHM of the Balmer lines remained relatively constant across the CL event. The emission lines of $OI\lambda 8446$ and $CaII\lambda\lambda 8498, 8542, 8662$ exhibit a double-peak structure (Ochmann et al. 2024), interpreted as sign of low turbulence and high column density in the region where they form.

The X-ray spectrum of NGC 1566 at outburst was measured in rapid follow-up observations with XMM-Newton, NuSTAR and Swift (Parker et al. 2019b). It is a typical type 1 X-ray spectrum at high-state, extending to high energies, and is modified by ionized absorption and mild reflection. With the reflection grating spectrometer (RGS) an outflow component with a velocity of 500 km/s, possibly launched during the outburst, was detected. The amount of X-ray cold absorption did not change between the low-state and high-state, rejecting variable (decreasing) absorption as the cause of the 2018 outburst. Parker et al. (2019b) concluded that a heating front propagating through the disk caused by the hydrogen ionization instability provides a consistent explanation of the outburst.

The Swift XRT long-term light curve of NGC 1566 (Parker et al. 2019b, Xu et al. 2024, our Fig. 3 including the latest 2024 observations) covers the decline phase of the 2018 outburst densely, but missed the rise phase.⁵ The latter was observed in the optical band with ASAS-SN (Dai et al. 2018) and was modeled by Kollatschny and Chelouche (2024) who preferred a lensing interpretation of the 2018 event.

⁵The long-term Swift BAT light curve does reveal another hard X-ray flare (Oh et al. 2018) in the year 2010, but that one was not followed up spectroscopically.

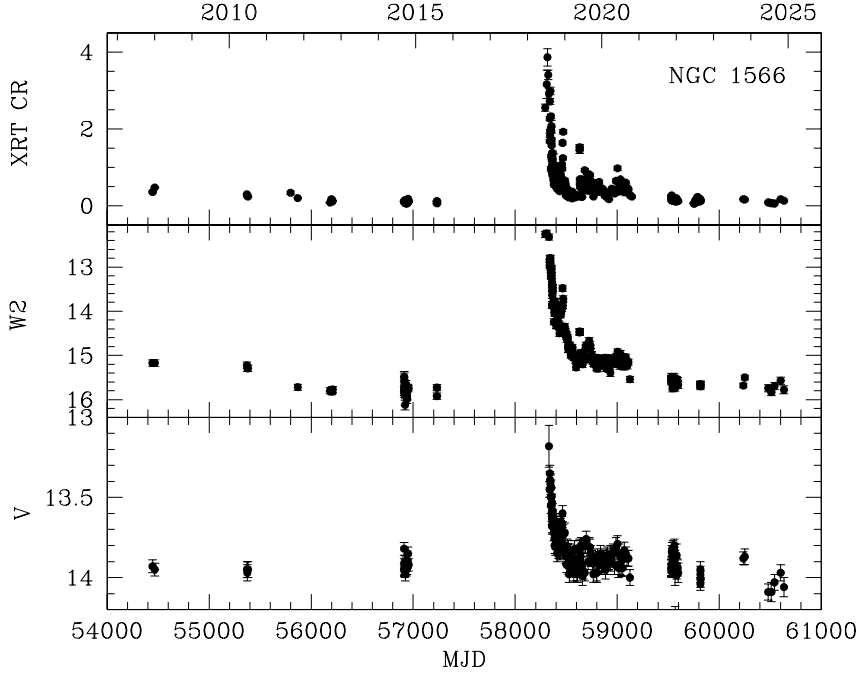


Fig. 3: Longterm Swift XRT and UVOT light curve of NGC 1566 until 2024. The X-ray count rate CR is given in counts/s, and the UV W2 and optical V magnitudes are reported in the VEGA system and are the directly observed values (not corrected for Galactic extinction). The last bright outburst of NGC 1566, accompanied by a CL event, happened in 2018.

The CL event of NGC 1566 is the nearest detected so far in NLS1 galaxies (Table 2), and NGC 1566 is among the nearest recurrent CL AGN known.

5.1.2. IC 3599

The Seyfert galaxy IC 3599 was among the most highly variable AGN detected in the ROSAT all-sky survey. Its X-ray brightness increased by more than a factor of 100 (among the AGN, significantly exceeded only by WPVS007 at that time; see below). The outburst, with an exceptionally soft X-ray spectrum, was accompanied by bright broad Balmer lines and high-ionization iron coronal lines (Brandt et al. 1995) which then faded strongly in the following years (Grupe et al. 1995b, Komossa and Bade 1999). The low-state spectra still show faint coronal lines, as well as a broad $H\alpha$ component implying a Seyfert 1.9 classification (Komossa and Bade 1999). Photoionization modeling of the optical outburst spectrum implied that the high-ionization lines are well explained with gas typical of a CLR, with a gas density of $\sim 10^9 \text{ cm}^{-3}$ (Komossa and Bade 1999). The origin of the CL event of IC 3599 was not discussed in more detail at that time, but an extreme case of NLS1 variability, a TDE, or an accretion-disk instability were briefly mentioned as possibilities (Brandt et al. 1995, Grupe et al. 1995b); the latter favored by Komossa and Bade (1999).

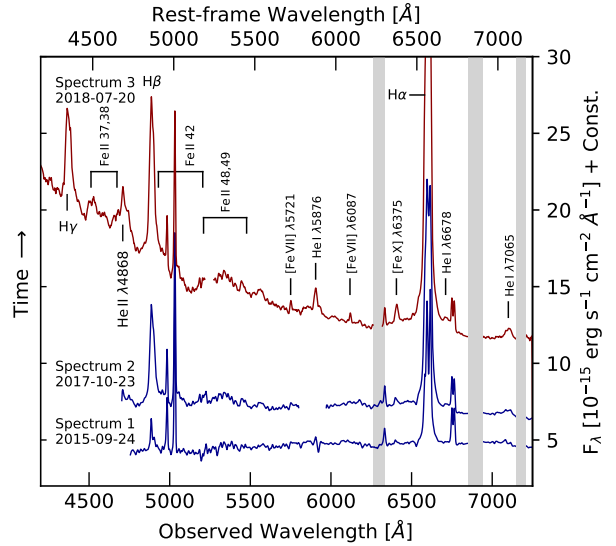


Fig. 4: Optical spectra of NGC 1566 showing its transition from a near type 2 AGN with only very faint broad Balmer lines of $H\alpha$ and $H\beta$ into a type 1 AGN during the strong continuum outburst in 2018. Adopted from Ochmann et al. (2024).

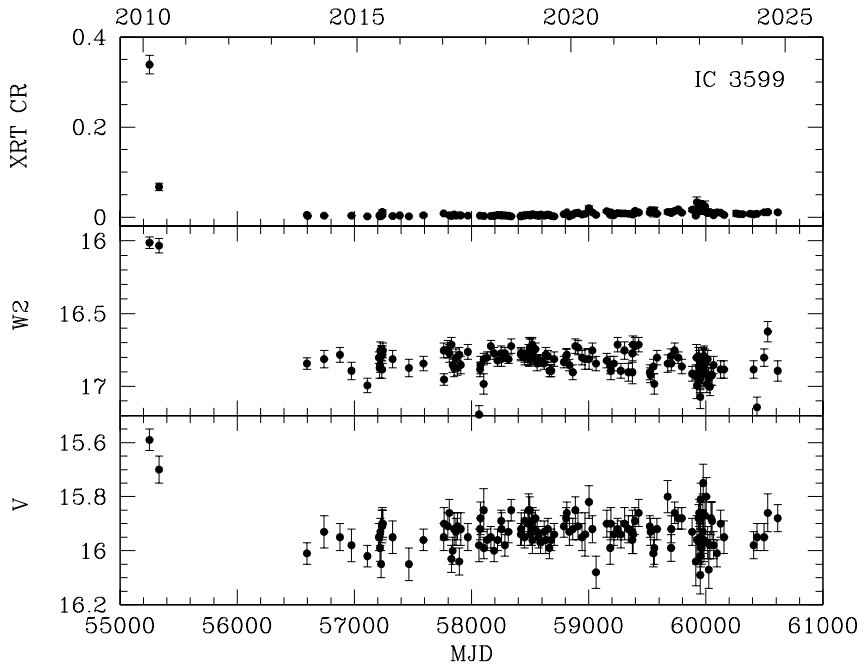


Fig. 5: Longterm Swift XRT and UVOT light curve of IC 3599 until 2024. The X-ray count rate CR is given in counts/s, and the UV W2 and optical V magnitudes are reported in the VEGA system and are the directly observed values (not corrected for Galactic extinction). The first of the two bright outbursts of IC 3599 was detected with ROSAT in 1990 and is not included in this plot. The second bright outburst was detected with Swift in 2010.

Unexpectedly, a second X-ray outburst of similar amplitude was detected in 2010 with Swift, 19.5 yr after the first one (Komossa et al. 2014, Campana et al. 2015, Grupe et al. 2015); unfortunately not accompanied by optical spectroscopy that time. A Lightman-Eardley disk instability was favored to explain the outburst behaviour. Using the observed outburst repeat time of 19.5 yrs and a SMBH mass in the range of $10^{6-7} M_{\odot}$ as determined from observations, implies a truncation radius between inner and outer disk of $r_{\text{trunc}} = 5-45 r_g$ (Grupe et al. 2015). No third outburst has so far been detected (Grupe et al. 2024), but significant lower-amplitude X-ray variability is ongoing (Fig. 5). The cause for the exceptional steepness of the X-ray outburst spectrum ($\Gamma_x \sim 4$) remains unknown, but it seems to imply the absence of an accretion disk corona. The X-ray spectrum remains supersoft in low-state as well.

Several features of IC 3599 remain surprising: In addition to the ultrasoft low-state X-ray spectrum, polarimetry (Grupe et al. 1998) did not reveal a high degree of optical polarization, and the supersoft X-ray outburst spectrum is inconsistent with strong cold absorption, implying that its Sy 1.9 nature in low-state is not due to severe extinction. Likely, just the BLR emission is intrinsically weak in the long-lasting low-states. The relatively stronger NLR emission could then be due to asymmetric radiation from the accretion disk and/or the AGN could have been brighter in the past and the NLR still reflects that previous state.

Swift continues to monitor this extreme optical CL AGN. Rapid multiwavelength follow-up studies including optical spectroscopy at dense cadence will provide us with a unique opportunity to measure the BLR and CLR response following the next giant outburst.

5.1.3. NGC 3516

The Seyfert galaxy NGC 3516 has long been known to be highly variable in its continuum and optical broad emission lines. NGC 3516 was part of the initial sample of Seyfert (1943). Strong broad-line variability was first noticed by Andrillat and Souffrin (1968). NGC 3516 stands out as highly variable in the X-ray band as well. It was one of the most highly variable AGN in a dedicated search for nearby such AGN in the ROSAT data base (Komossa and Bade 1999), and continues to show rapid and high-amplitude X-ray variability (Mehdipour et al. 2022). Its 2017 X-ray low-state was explained by a drop in intrinsic luminosity causing a decrease in the ionization state of the X-ray warm absorber as well (Mehdipour et al. 2022). Its long-term Swift XRT light curve until 2024 based on data retrieved from the Swift archive (Fig. 6) reveals epochs of correlated and uncorrelated optical and X-ray variability with very different SEDs (Fig. 7).

Optical spectroscopy of NGC 3516 at different activity states was obtained at numerous occasions over decades including dedicated BLR reverberation

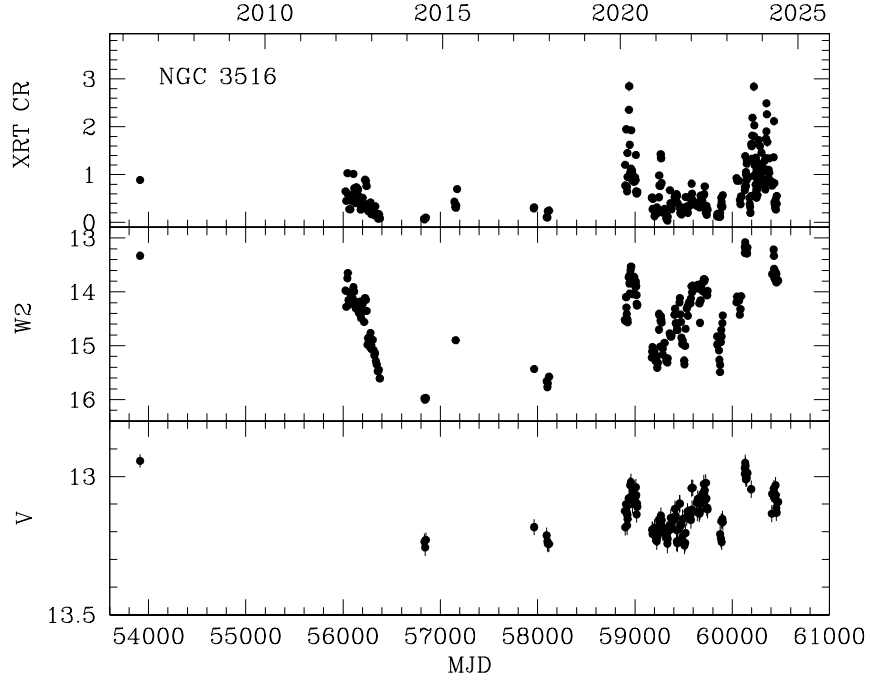


Fig. 6: Longterm Swift XRT and UVOT light curve of NGC 3516 until 2024. The X-ray count rate CR is given in counts/s, and the UV W2 and optical V magnitudes are reported in the VEGA system and are the directly observed values (not corrected for Galactic extinction). While the optical–UV is correlated with the X-rays at some epochs, they are independent at others.

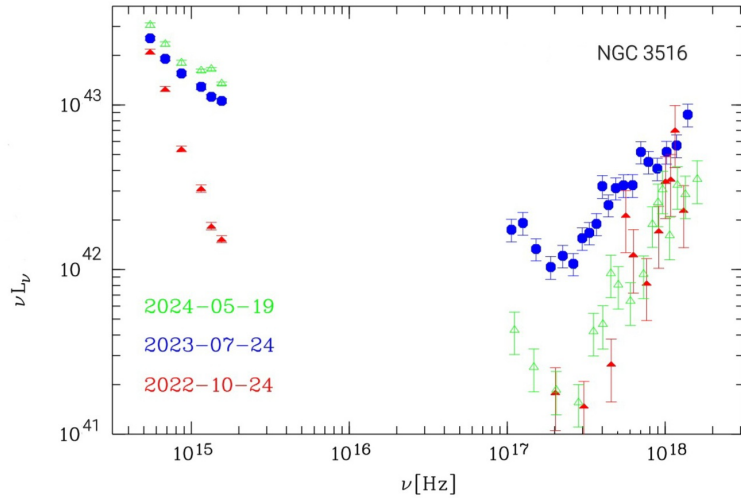


Fig. 7: Optical–UV–X-ray SEDs of NGC 3516 at three representative epochs, highlighting different variability behaviour: (1) the optical–UV high-state of May 2024 (open triangles; in green colour in the online version) is *not* accompanied by any X-ray high-state but rather a low-state; (2) the optical–UV high-state of July 2023 (filled circles; in blue colour in the online edition) is accompanied by an X-ray high-state, and (3) the optical low-state of October 2022 (filled triangles; in red colour in the online version) is accompanied by an X-ray low-state. The X-ray spectrum was corrected for Galactic absorption, and the optical–UV spectrum for Galactic extinction. The SEDs reveal the different optical–X-ray behaviour at different epochs.

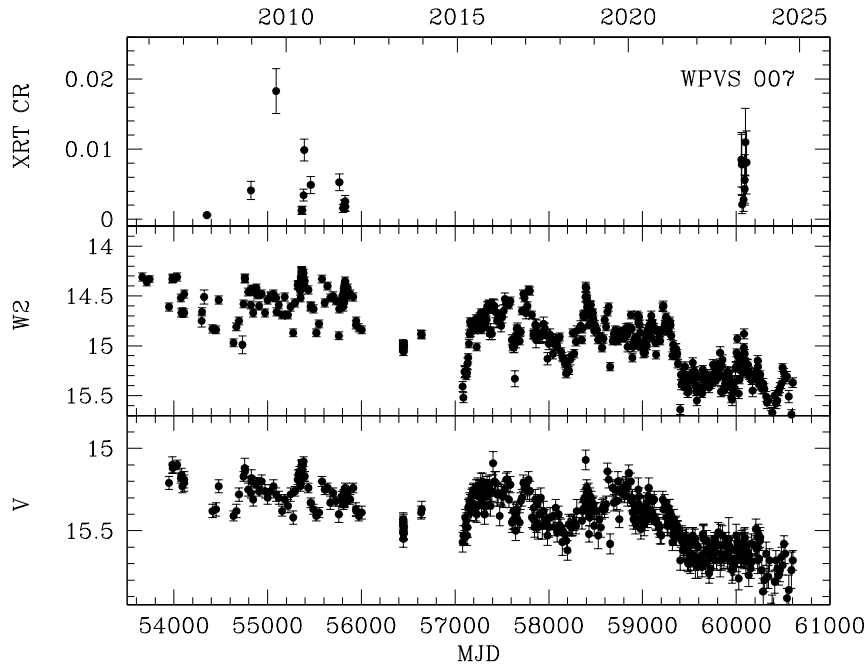


Fig. 8: Longterm Swift XRT and UVOT light curve of WPVS007 until 2024. The X-ray count rate CR is given in counts/s, and the UV W2 and optical V magnitudes are reported in the VEGA system and are the directly observed values (not corrected for Galactic extinction). Most of the time, WPVS007 is not detected in X-rays (upper limits not shown). WPVS007 is remarkable for its exceptional amplitude of variability in X-rays by a factor of ~ 400 (first detected with ROSAT; not included in this plot), interpreted as absorption event independently shown by the appearance of deep UV absorption lines. Since then, X-rays have only occasionally been detected in the Swift monitoring observations.

mapping campaigns (e.g. Wanders et al. 1993, Onken et al. 2003, Denney et al. 2010, Shapovalova et al. 2019, Ilić et al. 2020, Feng et al. 2021, Oknyansky et al. 2021, Popović et al. 2023, and references therein). These have confirmed that NGC 3516 is a CL AGN which varies strongly between type 1 and 1.9. The overall structure of the BLR does not change during low-states (Feng et al. 2021). Popović et al. (2023) concluded that an intrinsic mechanism rather than large-scale obscuration of the BLR is required to explain the CL events in NGC 3516, even though a contribution of dust within the BLR may still play a role at low activity states.

5.2. Other cases

5.2.1. WPVS007

The NLS1 galaxy WPVS 007 almost vanished from the X-ray sky ~ 35 years ago (Grupe et al. 1995a) after dropping by a factor of ~ 400 in flux. Its optical spectrum remained unchanged. UV spectroscopy with FUSE (Leighly et al. 2009) then revealed the cause of the X-ray faintness: the onset and development of a strong broad-absorption line (BAL) flow, remarkable for this low-mass galaxy, given that

BALs are predominantly observed in quasars (Laor and Brandt 2002). Occasionally, the X-rays flicker into brighter states detected with Swift (Fig. 8), but these episodes are rare and short-lived. The optical and UV continuum emission, highly variable in itself at small amplitude and interpreted as a mix of intrinsic variability and dust extinction at torus scales (Leighly et al. 2009, Li et al. 2019), continues to decline.

The variability of the highly ionized BAL outflow of WPVS007 with a large mass-loss rate and kinetic luminosity is well explained by a partial covering scenario, where the BAL outflow partially obscures the continuum source (Green et al. 2023). The recovery of WPVS007 in its brighter state is yet to come, and will provide us with an excellent opportunity of studying BAL processes on short timescales.

5.2.2. Mrk 335

Mrk 335 is a nearby, bright Seyfert galaxy, which has been observed with every major X-ray mission. Once among the X-ray brightest AGN, with Swift Mrk 335 was found in a historic minimum state (Grupe et al. 2007) in which it has spent most of the time since then, except for occasional flaring (Fig. 9).

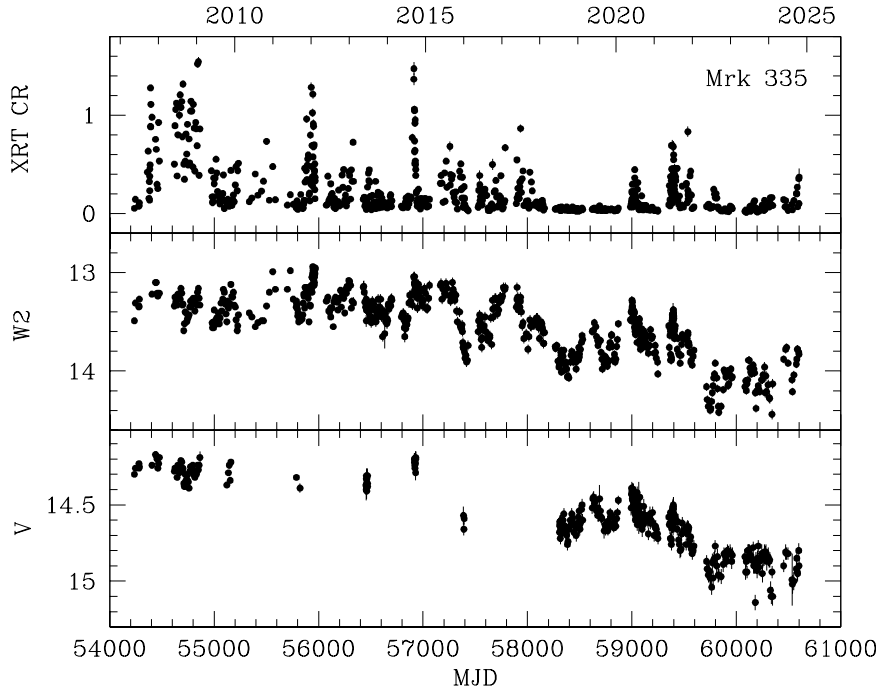


Fig. 9: Longterm Swift XRT and UVOT light curve of Mrk 335 until 2024. The X-ray count rate CR is given in counts/s, and the UV W2 and optical V magnitudes are reported in the VEGA system and are the directly observed values (not corrected for Galactic extinction). Once among the X-ray brightest AGN, Mrk 335 has remained in low-states most of the time in the last 1.5 decades, interrupted only by short-lived episodes of rapid flaring. These have become less frequent in recent years. For a duration of 2 years (2018–2020) the X-ray flaring ceased entirely. During the same time interval, the optical-UV emission continued to flare with similar amplitude as before.

The intermediate and low states are characterized by strong spectral complexity and were observed in several dedicated deep spectroscopic follow-ups, e.g. with XMM-Newton, Suzaku and NuSTAR (Grupe et al. 2012, Gallo et al. 2013, 2019, Parker et al. 2019a, Mondal and Stalin 2021, Ezhikode et al. 2021, Kara et al. 2023). Two very different types of spectral models provided equally successful X-ray spectral fits: partial-covering absorption, or a reflection model where the intrinsic photons are subject to blurred reflection from the inner accretion disk. The solution came from combining the X-ray with optical–UV data, revealing that the observed X-ray emission is uncorrelated with the observed optical–UV emission most of the time and at most timescales (Gallo et al. 2018, Komossa et al. 2020a, Kara et al. 2023) and that the high-ionization, broad HeII emission line does not follow the simultaneous high-amplitude X-ray variability despite the fact that HeII’s ionization potential lies in the soft X-ray regime (Komossa et al. 2020a). These results imply that the observed X-ray variability is predominantly caused by a (partial-covering, dust-free) absorber located mostly along our line-of-sight. The presence of line-of-sight absorption is independently detected in the form of narrow UV and X-ray absorption lines revealed with

HST (Longinotti et al. 2019) and with the RGS of XMM-Newton (Parker et al. 2019a, Liu et al. 2021). These results do not exclude a reflection contribution to the X-ray spectrum of Mrk 335, but show that a strong absorption component is required which drives at least a large fraction of the observed variability.

In summary, Mrk 335 is a good example for (dust-free) absorption-driven X-ray continuum variability. It is a frozen-look AGN as far as its broad HeII response to the observed X-ray emission is concerned (Komossa et al. 2020a). Its Hydrogen Balmer lines still do show a response to the mild optical continuum variability during the epoch when Mrk 335 was the target of reverberation mapping (Grier et al. 2012). Swift monitoring of Mrk 335 continues.

6. SEMI-PERIODIC VARIABILITY OF BINARY AGN AND BINARY SMBHs

6.1. Introduction

Binary SMBHs are the loudest sources of gravitational waves (GWs) in the Universe. They are in the frequency regime accessible by future space-based GW interferometers (in the millihertz regime) and by ongoing pulsar timing arrays (PTAs; in the nanohertz

regime). Binary SMBHs form and evolve in the course of galaxy mergers (Begelman et al. 1980). As the SMBHs undergo major episodes of accretion and ejection of matter, they not only grow substantially in mass and shape the galaxy core environment, but they also represent important multimessenger sources themselves. The field has received additional attention with the PTA discovery of a GW background (Arzoumanian et al. 2020), consistent with the signal from a population of massive binary SMBHs or alternatively implying physics beyond standard cosmology (see Verbiest et al. 2024, for a review). For all these reasons, an intense search for wide and close systems of binaries is ongoing. Systems in an early evolutionary stage and with large separations can still be spatially resolved [e.g. NGC 6240 in X-rays, J0402+379 in the radio, and SDSS J150243.1+111557 in the optical–radio regime (Komossa et al. 2003, Rodriguez et al. 2006, Fu et al. 2011)] at separations of pc to kpc scales. However, the most evolved, most compact systems, well beyond the final parsec in their evolution, can not yet be resolved even with powerful VLBI techniques, and we rely on indirect methods to search for them. Many such methods have been developed and scrutinized, and new ones continue to be proposed (see Komossa and Zensus 2016, De Rosa et al. 2019, D’Orazio and Charisi 2023, for reviews). In line with the topic of this review, we highlight the two most common ones. The first method is based on semi-periodic broad-line variability or other effects on the BLR structure. In particular, several models suggested to explain (individual) changing-look AGN have involved binary SMBHs. The second method makes use of (semi)-periodic variability of the broad-band continuum emission.

6.2. BLR signatures of binaries

If BLRs are separately bound to each of the two SMBHs of the binary in a galaxy merger, we expect to see a double-peaked or asymmetric broad-line profile from the two separate BLR contributions. Consequences of the presence of binaries on such BLR line profiles have been explored for decades, with focus on systematic variability of the red and blue wings of the BLR Balmer emission-line profiles representing Doppler shifts due to the orbital motion of the two SMBHs [(e.g. Gaskell 1983, Shen and Loeb 2010, Popović et al. 2021); review by Popović (2012)]. Since the variability timescales are of the order of decades, long-term optical spectroscopic monitoring is needed to identify such systems. Follow-ups of a few BLR double-peakers in the 1980s and 1990s did not detect any signs of orbital motion (Halpern and Eracleous 2000), and these AGN have been interpreted as systems with warped accretion disks or other processes around single SMBHs instead.

More recently, the large spectroscopic data base of SDSS has made it possible to identify large new samples of AGN with peculiar and/or double-peaked

Balmer-line profiles (e.g. Tsalmantza et al. 2011, Shen et al. 2013, Ju et al. 2013). So far, no binary SMBH has been uniquely identified this way, because the majority of line-profile variations observed in years of spectroscopic monitoring did not show the expected orbital modulation (Runnoe et al. 2017, Wang et al. 2017). A few candidate binaries remain in these samples.

Other approaches have explored different effects of a binary’s presence on the BLR emission: If a TDE happens at the secondary SMBH in a binary SMBH system, the non-central illumination of the circumbinary disk implies strong asymmetries in the disk response, evident in the velocity-delay maps (Brem et al. 2014). If only the secondary (lower-mass) SMBH in a binary system is highly accreting and has a BLR, its orbital motion will be imprinted in the (single-peaked) broad-line profile (Simić et al. 2022). In another approach, Savić et al. (2019), Marin et al. (2023) proposed the method of polarimetry and polarimetric reverberation mapping to distinguish between binary SMBHs and gas/dust physics as cause of complex BLR line profiles. Shocks produced when a secondary black hole is crossing the disk around a primary could produce highly variable, kinematically shifting extra components in the Balmer lines, as observed in NGC 5548 (Shapovalova et al. 2004, Bon et al. 2016).

Finally, the presence of binary SMBHs has also been suggested to be among the mechanisms to produce CL AGN (Section 2). Wang and Bon (2020) explored a scenario where close binaries on eccentric orbits are able to trigger a CL transition through tidal torques affecting the mini-disk(s) of the system. Zrake et al. (2024) have shown that effects on the accretion disk during advanced stages of GW driven inspirals of binary SMBHs can produce CL AGN and applied their model to the case of Mrk 1018 which transitioned between type 1 and 1.9.

6.3. Semi-periodic light curve variability

This binary SMBH search method makes use of (semi)-periodic signals in long-term multiwavelength light curves. These signals can arise either as a consequence of orbital motion of one or both SMBHs, or precession of the accretion disk or jet. At least several periods should be covered in any light curve to represent a reliable detection; otherwise noise can mimic the periodic signal (Vaughan et al. 2016).

Many recent searches for binary SMBH candidates have been conducted on optical photometric surveys such as the Catalina Real-time Transient Survey (CRTS; Graham et al. 2015a), the Palomar Transient Factory (PTF; Charisi et al. 2016), Pan-STARRS (Liu et al. 2016), DES-SN/SDSS-S82 (Chen et al. 2020), and the ZTF (Chen et al. 2024), among these the well-studied system PG 1302–102 (e.g. Graham et al. 2015b, D’Orazio et al. 2015, Kovačević et al. 2019).

In addition to dedicated searches in large-area sky surveys, numerous single AGN have been identified as candidate binaries in recent years based on their light curve characteristics [e.g. PKS 2131–021 (Ren et al. 2021) with sinusoidal flux variability in the radio band, Tick-Tock (SDSS J143016.05+230344.4) with initial indications of a decreasing period in its optical light curve (Jiang et al. 2022, Dotti et al. 2023), and evidence for periodic optical flux and line variability of NGC 5548 (Bon et al. 2016), and references therein].

A different semi-periodic light curve pattern, not sinusoidal, is shown by the candidate binary SMBH OJ 287. Its long-term optical light curve exhibits recurrent bright double-peaked outbursts repeating every $\sim 11 \pm 1$ yrs (with a separation between the two peaks of ~ 1 yr), most clearly present in the 1970–1990 light curve of this blazar (see Fig. 1 of Valtaoja et al. 2000). The most recent double-peak has been identified in 2016–2017 (Komossa et al. 2023b). OJ 287 has the most densely covered multi-frequency light curve of all binary SMBH candidates (Komossa et al. 2021a, 2023b) and is discussed in more detail in the next Section.

6.4. The case of OJ 287

Very different variants of binary SMBH models for OJ 287 have been explored in the literature. These involved either jet or disk precession, orbital motion of one or two jet-emitting SMBHs, impacts of the orbiting secondary SMBH on the disk around the primary SMBH or more indirect effects on the primary’s disk, or the presence of mini-disks around two SMBHs fed by a circum-binary disk (Sillanpaa et al. 1988, Lehto and Valtonen 1996, Katz 1997, Villata et al. 1998, Valtaoja et al. 2000, Liu and Wu 2002, Britzen et al. 2018, Tanaka 2013). According to other suggestions, a binary is not required, or its absence is preferred (Villforth et al. 2010, Butuzova and Pushkarev 2020). Almost all of the binary scenarios have offered potential explanations for the double-peaked nature of the outbursts and were based on excellent theoretical frame works. However, none of those which attempted a detailed prediction at that time then matched the observed 2005–2007 outburst timings. One of the models, the one requiring a large primary SMBH mass of $> 10^{10} M_{\odot}$, was refined and updated, and then high-accuracy predictions of the next flare epochs for the years 2021–2022 were published (Valtonen et al. 2022). That model is referred to as the precessing binary (PB) model hereafter. However, none of the outbursts predicted with small uncertainties in the period 2021–2022 were observed. That period was densely covered by a newly initiated OJ 287 program, MOMO (Multiwavelength Observations and Modeling of OJ 287) that started in 2015 (e.g. Komossa et al. 2023c). MOMO is designed to distinguish between different binary SMBH scenarios, and it independently probes blazar disk-jet physics. Dense monitoring of OJ 287 at a ca-

dence of a day to weeks at multiple frequencies in the radio, optical, UV, X-ray and gamma-ray bands, along with dedicated deeper multiwavelength follow-up spectroscopy at selected epochs, provides timing, spectra, and broadband SEDs at all activity states of OJ 287 (e.g. Komossa et al. 2017, 2020b, 2021b,a, 2023b). This is the densest and longest multiwavelength monitoring program so far carried of OJ 287 at > 12 frequencies, and among the densest of any blazar (Fig. 10).

MOMO covered the latest epochs of outbursts, predicted by the PB model, densely: first, a precursor flare was predicted to occur in December 2021, and second, the time of the big main outburst was predicted to be ‘October 10, 2022, ± 10 days’ (Valtonen et al. 2022, their Section 4). However, none showed up. OJ 287 remained at low activity levels at both epochs and before and after, up until to date. Instead, the last big double-peaked outburst of OJ 287 was observed in 2016–2017 (Komossa et al. 2017, 2023b, our Fig. 10).⁶ Further, none of the other key parameters of that binary model were confirmed, including the large SMBH mass and the corresponding high accretion rate implying a high accretion luminosity: the model luminosity overpredicts by a factor of > 10 –100 the upper limit on the actually measured disk luminosity in OJ 287’s low-states. Further, the actually measured (primary) SMBH mass, based on the BLR single-epoch relation, among the best-established methods to routinely measure the SMBH masses of AGN (Vestergaard and Peterson 2006), implies a (primary) SMBH mass of OJ 287 a factor of ~ 100 lower than required by the PB model: Komossa et al. (2023a) measured $10^8 M_{\odot}$ of the (primary) SMBH of OJ 287. Finally, the required Bremsstrahlung emission was not observed either. The PB model required the blazar spectrum to jump from blazar synchrotron emission to a Bremsstrahlung spectrum at outburst epochs with a very different spectral shape. That was not observed, neither in recent years Komossa et al. (2023c,b), nor during previous outburst epochs (Gopal-Krishna 2024). These multiple independent arguments and direct measurements have ruled out the PB model.⁷ OJ 287 may still be a binary SMBH, but then in an entirely different parameter regime.

⁶That outburst (possibly already starting in December 2015) was the last big observed outburst (a factor of ~ 10 in flux) since 2007; the ‘Spitzer flare’ of 2019 (Laine et al. 2020) was of low amplitude (30% in flux), similar to other low-level flaring detected every year and, therefore, due to similar processes related to the variable blazar jet emission of OJ 287.

⁷These results from recent years also rule out speculations from 2024 about a dark matter spike near OJ 287 (Chan and Lee 2024), because these speculations were still based on the old PB model. Any claim of a dark matter halo of OJ 287 has to be re-evaluated based on up-to-date binary parameters including the measured primary SMBH mass.

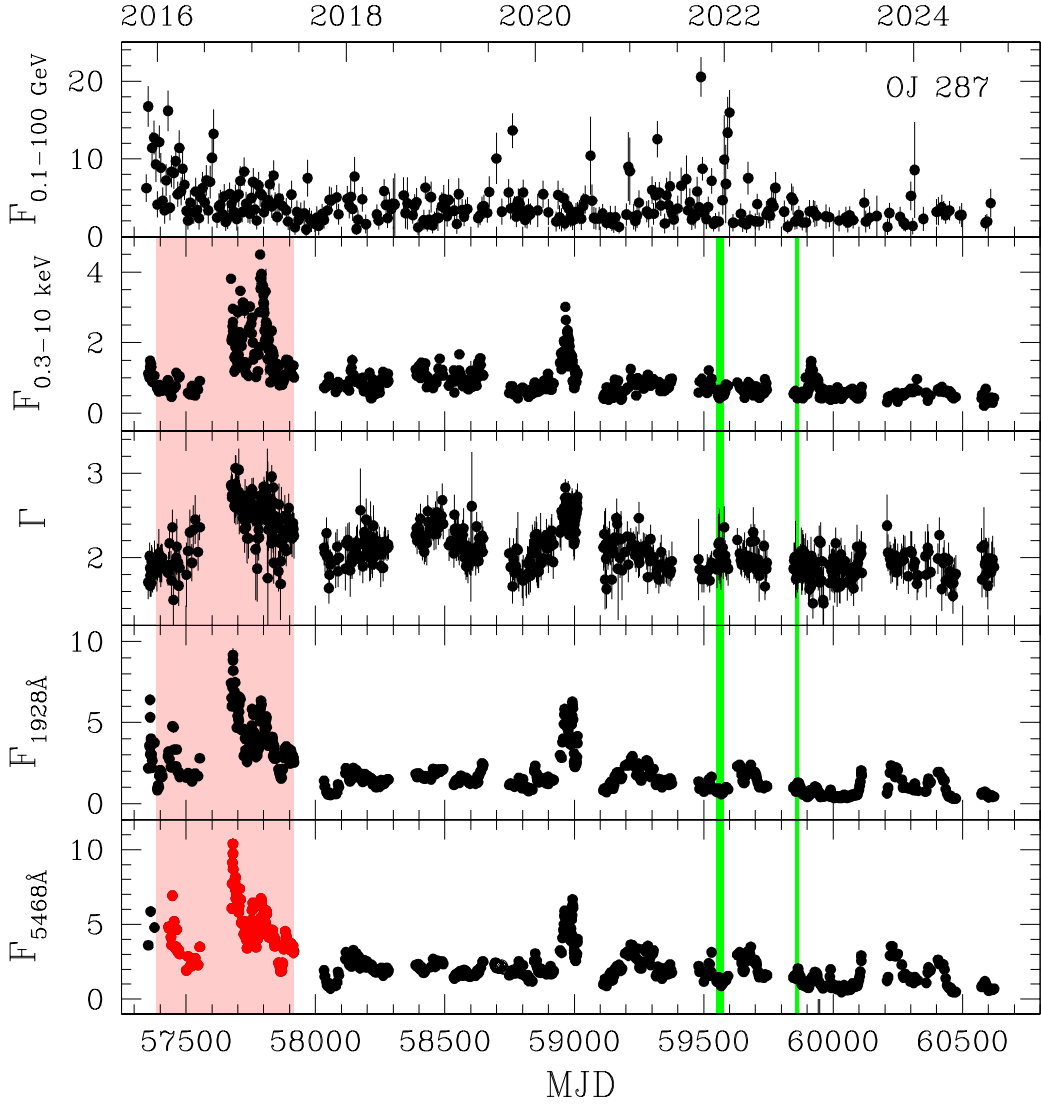


Fig. 10: Swift MOMO and Fermi light curve of OJ 287 between late 2015 and 2024 [from top to bottom: gamma-ray flux measured by Fermi (the highest data point from 2015 is off the plot, and only detections are shown, no upper limits), absorption-corrected Swift (0.3–10 keV) X-ray flux, X-ray photon spectral index, Swift UVOT UV W2 flux at 1928Å, and Swift V flux at 5468Å. Fluxes are reported in units of 10^{-11} erg/cm²/s and were corrected for Galactic extinction. The epochs of two *optical* (thermal Bremsstrahlung) outbursts predicted by one of the binary SMBH models (a precursor flare in 2021 and a main outburst in 2022) are marked with grey vertical lines (green in the online version). The predicted optical outbursts did not show up; rather the emission was at low levels at these epochs, ruling out the model which made these predictions. Instead, the last optical double-peaked outburst was observed in 2016–2017 (marked in grey, or red in the online version).

The long-term light curve of OJ 287 at selected MOMO frequencies since the start of the project is shown in Fig. 10. Previously unpublished Swift X-ray, optical, and UV measurements of 2024 from the MOMO project are included, as well as gamma-ray measurements from the Fermi satellite (Abdollahi et al. 2023). The absence of any outburst activity at the epochs predicted by the PB model in 2021 and 2022 (green vertical lines) is immediately evi-

dent. OJ 287 continues to be at low emission levels at all frequencies throughout 2024. The last bright double-peaked optical outburst (marked in red) was detected in 2016–2017.

The next double-peak is expected in the time frame 2026–2028 (Komossa et al. 2023b), and dense monitoring in the course of the MOMO project is planned.

In summary, successful future binary SMBH models of OJ 287 should reproduce a regular double peak every ~ 11 yr allowing for ± 1 yr variations, should be based on a moderate primary SMBH mass of $\sim 10^8 M_\odot$, and should reproduce synchrotron outbursts. One promising future approach will be the application of recent binary merger simulations which predict SMBH binaries with mini-disks fed by a larger circum-binary disk (D’Orazio et al. 2013). Tanaka (2013) loosely suggested that such a scenario could hold for OJ 287, but detailed modeling of OJ 287 within that framework has not yet been carried out.

The low measured SMBH mass implies that any GWs from OJ 287 are no longer in the sensitivity regime of near-future PTAs (at higher primary SMBH mass, OJ 287 might have been detectable with SKA-II; Yardley et al. 2010). Rather, OJ 287 would be a precursor of systems detectable upon their final coalescence with LISA-type space-based GW interferometers (Colpi et al. 2019).

7. OPEN QUESTIONS AND FUTURE PROSPECTS

The phenomenon of CL AGN is not new, but the identification of large numbers of these events and in luminous quasars as well has motivated many important new theoretical studies of rapid accretion-disk structural and flux changes. On the modeling side, more predictions are still needed for the actual variability timescales, and the resulting spectral shape of the emission and its evolution in order to facilitate a rigorous comparison with observations. Often, this is still challenging due to the large number of free parameters and/or the non-analytic approach in form of simulations.

Another important question, little explored so far, should address if and how jets are formed during the CL events in AGN (Yang et al. 2021), and/or how the existing jets are affected. Much denser radio monitoring observations of the nearby Seyfert galaxies are required to search for variability and morphological changes in compact jets in order to assess if such features are persistently compact or have been newly launched in the course of the CL event, for instance.

A more homogeneous search and classification scheme of CL AGN would be useful, especially involving a well-defined minimum factor of variability to call an event a CL AGN. Hundredths of CL AGN have been identified by now, and the transition between lower-amplitude variability as frequently traced by classical reverberation mapping (often a factor of 2 or less) and the larger-amplitude outbursts is rather smooth, so the classification of CL AGN is not yet unique in the literature; a factor-of-2 BLR variability is considered ‘normal AGN variability’ by some, but a CL AGN by others.

Upcoming time domain surveys in the optical and X-ray bands will not only detect large numbers of

new extremely variable AGN and CL AGN, but will also facilitate a search for the characteristic periodic signals of binary SMBHs based on high-cadence light curves coverage. In the optical bands, the Vera C. Rubin Observatory Legacy Survey of Space and Time (LSST; Ivezić et al. 2019) is scheduled to start operation in the year 2025. While photometric surveys will detect outstanding numbers of new transients, spectroscopic follow-ups will be crucial to identify CL AGN. This includes a rapid response in cases of the low-mass SMBHs. For example, in case of a $10^6 M_\odot$ SMBH, the BLR will be crossed in days and a response time of hours to days and high cadence every few hours is required to follow the line response across the whole BLR.

A major challenge will be to distinguish true CLs from impostors (Section 4) in the absence of dense spectroscopic follow-ups. More look-alikes like extreme SNe will be found, therefore we need more ways to distinguish quickly, ideally already from photometry, or involving X-rays.

Longer-term spectroscopic monitoring at high sensitivity is of interest to detect and map the inner CLR as well. Only a few systems with highly variable coronal lines have so far been detected (Section 5), and reverberation mapping of the CLR has not yet been carried out.

Finally, regarding binary SMBHs, the case of OJ 287 has particularly demonstrated, how challenging it is to identify even good candidate systems, and much more so to pin down their binary nature. LSST (e.g. Ivezić et al. 2019, Kovačević et al. 2021, Xin and Haiman 2021, Bianco et al. 2022, Kovačević et al. 2022) will play an important role in identifying more candidate binary AGN with well-covered light curves of high cadence, especially in the regime of orbital periods less than few years. While the high cadence of LSST implies that it can find shorter periods, its high sensitivity implies that it will cover AGN with lower-mass binaries, of which there are many more. Therefore, the LSST catalog will contain large numbers of fainter short-period binaries. The most evolved, ultra-compact, SMBH binaries with periods of only days which then coalesce years later in the LISA time window, can be detected in the optical band with LSST through the periodic light-curve modulation from the circum-binary disk feeding the two SMBH’s mini-disks (Xin and Haiman 2024). The orbital modulation from the two mini-disks themselves is best searched for in the X-ray regime, for instance with the newly launched mission SVOM (Wei et al. 2016), given the compactness of the mini-disks at very advanced stages of binary merger evolution.

Finally, with the PTA searches becoming increasingly sensitive (Verbiest et al. 2024), the detection of GWs from single binary SMBHs is on the horizon, either through the discovery of previously unknown binaries, or through targeted PTA searches of known binary candidates.

8. SUMMARY AND CONCLUSIONS

The extremes of AGN variability represent a transformative frontier in astrophysics. So far, only a small number of well-studied, well-monitored CL events have been modeled in detail, but the favored scenarios differ from source to source. Larger samples and rigorous modeling will be crucial to fully understand accretion physics and the central engine of AGN. The study of CL events in different subtypes of AGN beyond BLS1s is still largely unexplored. Understanding the CL events across the whole AGN population, from NLS1 galaxies at low SMBH masses and in the high-accretion regime, to LINERs at high SMBH masses and in the low accretion regime, still in its infancy, will provide a unique new probe of the extremes of the accretion regimes in AGN.

The search for binary SMBHs (especially via BLR profiles and semi-periodic continuum variability), as important as it is for multimessenger astrophysics, has turned out to be challenging, and no spatially unresolved binary SMBH has been uniquely identified so far, even though many candidates have been found during the last decade. GW detection of single systems with PTAs or space-based GW interferometers will be an important step, and may be the only way to uniquely identify binaries in the near future. The leading model for the best-known binary candidate, OJ 287, has been ruled out in recent years based on multiple independent arguments and measurements from the MOMO project, and new binary modeling is required which has to account for the measured low (primary) SMBH mass of $10^8 M_{\odot}$, and the presence or absence of outbursts in recent years, with the last big outburst observed in 2016–2017. The low primary SMBH mass of OJ 287 also has implications for future attempts to resolve the system spatially (e.g. with ngEHT), for the spatial scales in the jet that EHT will be able to resolve, and for its possible GW detection (if a binary interpretation holds): OJ 287 will no longer be in the regime of near-future PTAs but is rather a precursor to systems detectable with the future space-based GW interferometer LISA. Upcoming time domain surveys will greatly increase the number of binary SMBH candidates at periods of weeks to years. Ultimate confirmations of candidate systems may have to await the detection of GW emission with PTAs and/or with the first generation of space-based GW interferometers, and will then initiate a new era of multimessenger astrophysics.

Acknowledgements – We would like to thank the Swift team for carrying out the observations we proposed. In addition to our own data, we have also used the Swift archive at <https://swift.gsfc.nasa.gov/archive/>. We would like to thank W. Kollatschny, M. Ochmann, L. Popović, and J. Wang for permission to use their figures. This research was supported in part by grant NSF PHY-2309135 to the Kavli Institute for Theoretical Physics (KITP).

This work made use of data supplied by the UK Swift Science Data Centre at the University of Leicester (Evans et al. 2007). This work has made use of public Fermi-LAT data (Abdollahi et al. 2023). This research has made use of the XRT Data Analysis Software (XRTDAS) developed under the responsibility of the ASI Science Data Center (ASDC), Italy. This work has also made use of the NASA Astrophysics Data System Abstract Service (ADS), and the NASA/IPAC Extragalactic Database (NED) which is operated by the Jet Propulsion Laboratory, California Institute of Technology, under contract with the National Aeronautics and Space Administration.

REFERENCES

- Abdollahi, S., Ajello, M., Baldini, L., et al. 2023, *ApJS*, **265**, 31
- Alloin, D., Pelat, D., Phillips, M. and Whittle, M. 1985, *ApJ*, **288**, 205
- Alloin, D., Pelat, D., Phillips, M. M., Fosbury, R. A. E. and Freeman, K. 1986, *ApJ*, **308**, 23
- Anderson, K. S. and Kraft, R. P. 1969, *ApJ*, **158**, 859
- Andrillat, Y. and Souffrin, S. 1968, *ApL*, **1**, 111
- Arzoumanian, Z., Baker, P. T., Blumer, H., et al. 2020, *ApJL*, **905**, L34
- Begelman, M. C., Blandford, R. D. and Rees, M. J. 1980, *Natur*, **287**, 307
- Bianco, F. B., Ivezić, Ž., Jones, R. L., et al. 2022, *ApJS*, **258**, 1
- Blanchard, P. K., Nicholl, M., Berger, E., et al. 2017, *ApJ*, **843**, 106
- Blandford, R. D. and McKee, C. F. 1982, *ApJ*, **255**, 419
- Bon, E., Zucker, S., Netzer, H., et al. 2016, *ApJS*, **225**, 29
- Boroson, T. A. 2002, *ApJ*, **565**, 78
- Boroson, T. A. and Green, R. F. 1992, *ApJS*, **80**, 109
- Brandt, W. N., Pounds, K. A. and Fink, H. 1995, *MNRAS*, **273**, L47
- Brem, P., Cuadra, J., Amaro-Seoane, P. and Komossa, S. 2014, *ApJ*, **792**, 100
- Britzen, S., Fendt, C., Witzel, G., et al. 2018, *MNRAS*, **478**, 3199
- Burrows, D. N., Hill, J. E., Nousek, J. A., et al. 2005, *SSRv*, **120**, 165
- Butuzova, M. S. and Pushkarev, A. B. 2020, *Univ*, **6**, 191
- Campana, S., Mainetti, D., Colpi, M., et al. 2015, *A&A*, **581**, A17
- Cao, X., You, B. and Wei, X. 2023, *MNRAS*, **526**, 2331
- Chan, M. H. and Lee, C. M. 2024, *ApJL*, **962**, L40
- Charisi, M., Bartos, I., Haiman, Z., et al. 2016, *MNRAS*, **463**, 2145
- Chavushyan, V., Patiño-Álvarez, V. M., Amaya-Almazán, R. A. and Carrasco, L. 2020, *ApJ*, **891**, 68
- Chen, Y.-C., Liu, X., Liao, W.-T., et al. 2020, *MNRAS*, **499**, 2245
- Chen, Y.-J., Zhai, S., Liu, J.-R., et al. 2024, *MNRAS*, **527**, 12154
- Cohen, R. D., Rudy, R. J., Puetter, R. C., Ake, T. B. and Foltz, C. B. 1986, *ApJ*, **311**, 135

- Colpi, M., Holley-Bockelmann, K., Bogdanovic, T., et al. 2019, arXiv e-prints, (DOI: 10.48550/arXiv.1903.06867), arXiv:1903.06867
- da Silva, P., Steiner, J. E. and Menezes, R. B. 2017, *MNRAS*, **470**, 3850
- Dai, X., Stanek, K. Z., Kochanek, C. S., Shappee, B. J. and ASAS-SN Collaboration. 2018, *ATel*, **11893**, 1
- De Rosa, A., Vignali, C., Bogdanović, T., et al. 2019, *NewAR*, **86**, 101525
- Denney, K. D., Peterson, B. M., Pogge, R. W., et al. 2010, *ApJ*, **721**, 715
- Denney, K. D., De Rosa, G., Croxall, K., et al. 2014, *ApJ*, **796**, 134
- Dexter, J. and Begelman, M. C. 2019, *MNRAS*, **483**, L17
- Dong, Q., Zhang, Z.-X., Gu, W.-M., Sun, M. and Zheng, Y.-G. 2024, arXiv e-prints, (DOI: 10.48550/arXiv.2408.07335), arXiv:2408.07335
- Dong, S., Chen, P., Bose, S., et al. 2016, *ATel*, **9843**, 1
- D’Orazio, D. J. and Charisi, M. 2023, arXiv e-prints, (DOI: 10.48550/arXiv.2310.16896), arXiv:2310.16896
- D’Orazio, D. J., Haiman, Z. and MacFadyen, A. 2013, *MNRAS*, **436**, 2997
- D’Orazio, D. J., Haiman, Z. and Schiminovich, D. 2015, *Natur*, **525**, 351
- Dotti, M., Bonetti, M., Rigamonti, F., et al. 2023, *MNRAS*, **518**, 4172
- Ducci, L., Siebert, T., Diehl, R., et al. 2018, *ATel*, **11754**, 1
- Edelson, R., Gelbord, J., Cackett, E., et al. 2019, *ApJ*, **870**, 123
- Evans, P. A., Beardmore, A. P., Page, K. L., et al. 2007, *A&A*, **469**, 379
- Ezhikode, S. H., Dewangan, G. C. and Misra, R. 2021, *Journal of Astrophysics and Astronomy*, **42**, 51
- Feng, H.-C., Hu, C., Li, S.-S., et al. 2021, *ApJ*, **909**, 18
- Fian, C., Mediavilla, E., Motta, V., et al. 2021, *A&A*, **653**, A109
- Forman, W., Jones, C., Cominsky, L., et al. 1978, *ApJS*, **38**, 357
- Foschini, L., Lister, M. L., Antón, S., et al. 2021, *Univ*, **7**, 372
- Frederick, S., Gezari, S., Graham, M. J., et al. 2019, *ApJ*, **883**, 31
- Fu, H., Zhang, Z.-Y., Assef, R. J., et al. 2011, *ApJL*, **740**, L44
- Gallo, L. C., Fabian, A. C., Grupe, D., et al. 2013, *MNRAS*, **428**, 1191
- Gallo, L. C., Blue, D. M., Grupe, D., Komossa, S. and Wilkins, D. R. 2018, *MNRAS*, **478**, 2557
- Gallo, L. C., Gonzalez, A. G., Waddell, S. G. H., et al. 2019, *MNRAS*, **484**, 4287
- Gaskell, C. M. 1983, in *Liege International Astrophysical Colloquia*, Vol. 24, Liege International Astrophysical Colloquia, ed. J.-P. Swings, 473–477
- Gaskell, C. M. and Harrington, P. Z. 2018, *MNRAS*, **478**, 1660
- Gaskell, C. M. and Sparke, L. S. 1986, *ApJ*, **305**, 175
- Gehrels, N., Chincarini, G., Giommi, P., et al. 2004, *ApJ*, **611**, 1005
- Goodrich, R. W. 1989, *ApJ*, **342**, 224
- Gopal-Krishna. 2024, *A&A*, **688**, L16
- Graham, A. W. 2016, in *Astrophysics and Space Science Library*, Vol. 418, Galactic Bulges, ed. E. Laurikainen, R. Peletier and D. Gadotti, 263
- Graham, M. J., Djorgovski, S. G., Stern, D., et al. 2015a, *MNRAS*, **453**, 1562
- Graham, M. J., Djorgovski, S. G., Stern, D., et al. 2015b, *Natur*, **518**, 74
- Graham, M. J., Ross, N. P., Stern, D., et al. 2020, *MNRAS*, **491**, 4925
- Green, K. S., Gallagher, S. C., Leighly, K. M., et al. 2023, *ApJ*, **953**, 186
- Green, P. J., Pulgarin-Duque, L., Anderson, S. F., et al. 2022, *ApJ*, **933**, 180
- Grier, C. J., Peterson, B. M., Pogge, R. W., et al. 2012, *ApJL*, **744**, L4
- Grupe, D. 2004, *AJ*, **127**, 1799
- Grupe, D., Beuerman, K., Mannheim, K., et al. 1995a, *A&A*, **300**, L21
- Grupe, D., Beuermann, K., Mannheim, K., et al. 1995b, *A&A*, **299**, L5
- Grupe, D., Wills, B. J., Wills, D. and Beuermann, K., 1998, *A&A*, **333**, 827G
- Grupe, D., Komossa, S. and Gallo, L. C. 2007, *ApJL*, **668**, L111
- Grupe, D., Komossa, S., Gallo, L. C., et al. 2012, *ApJS*, **199**, 28
- Grupe, D., Komossa, S. and Saxton, R. 2015, *ApJL*, **803**, L28
- Grupe, D., Komossa, S. and Wolsing, S. 2024, *ApJ*, **969**, 98
- Guo, W.-J., Zou, H., Fawcett, V. A., et al. 2024, *ApJS*, **270**, 26
- Halpern, J. P. and Eracleous, M. 2000, *ApJ*, **531**, 647
- Hon, W. J., Wolf, C., Onken, C. A., Webster, R. and Auchettl, K. 2022, *MNRAS*, **511**, 54
- Hutsemékers, D., Agís González, B., Marin, F., et al. 2019, *A&A*, **625**, A54
- Ilić, D., Oknyansky, V., Popović, L. Č., et al. 2020, *A&A*, **638**, A13
- Ivezić, Ž., Kahn, S. M., Tyson, J. A., et al. 2019, *ApJ*, **873**, 111
- Jiang, N., Wang, T., Dou, L., et al. 2021, *ApJS*, **252**, 32
- Jiang, N., Yang, H., Wang, T., et al. 2022, arXiv e-prints, (DOI: 10.48550/arXiv.2201.11633), arXiv:2201.11633
- Ju, W., Greene, J. E., Rafikov, R. R., Bickerton, S. J. and Badenes, C. 2013, *ApJ*, **777**, 44
- Kaaz, N., Liska, M. T. P., Jacquemin-Ide, J., et al. 2023, *ApJ*, **955**, 72
- Kara, E., Barth, A. J., Cackett, E. M., et al. 2023, *ApJ*, **947**, 62
- Katz, J. I. 1997, *ApJ*, **478**, 527
- Kielkopf, J., Brashear, R. and Lattis, J. 1985, *ApJ*, **299**, 865
- Kollatschny, W. and Chelouche, D. 2024, *A&A*, **690**, L2
- Kollatschny, W. and Fricke, K. J. 1985, *A&A*, **146**, L11
- Kollatschny, W., Grupe, D., Parker, M. L., et al. 2020, *A&A*, **638**, A91

- Kollatschny, W., Grupe, D., Parker, M. L., et al. 2023, *A&A*, **670**, A103
- Kollmeier, J., Anderson, S. F., Blanc, G. A., et al. 2019, in *Bulletin of the American Astronomical Society*, Vol. 51, 274
- Komossa, S. 2015, *JHEAp*, **7**, 148
- Komossa, S. and Bade, N. 1999, *A&A*, **343**, 775
- Komossa, S. and Zensus, J. A. 2016, in *Star Clusters and Black Holes in Galaxies across Cosmic Time*, ed. Y. Meiron, S. Li, F. K. Liu, and R. Spurzem, Vol. 312, 13–25
- Komossa, S., Burwitz, V., Hasinger, G., et al. 2003, *ApJL*, **582**, L15
- Komossa, S., Zhou, H., Rau, A., et al. 2009, *ApJ*, **701**, 105
- Komossa, S., Grupe, D., Saxton, R. and Gallo, L. 2014, in *Proceedings of Swift: 10 Years of Discovery (SWIFT 10)*, 143
- Komossa, S., Grupe, D., Schartel, N., et al. 2017, in *IAU Symposium*, Vol. 324, *New Frontiers in Black Hole Astrophysics*, ed. A. Gomboc, 168–171
- Komossa, S., Grupe, D., Gallo, L. C., et al. 2020a, *A&A*, **643**, L7
- Komossa, S., Grupe, D., Parker, M. L., et al. 2020b, *MNRAS*, **498**, L35
- Komossa, S., Grupe, D., Gallo, L. C., et al. 2021a, *ApJ*, **923**, 51
- Komossa, S., Grupe, D., Parker, M. L., et al. 2021b, *MNRAS*, **504**, 5575
- Komossa, S., Grupe, D., Kraus, A., et al. 2023a, *MNRAS*, **522**, L84
- Komossa, S., Kraus, A., Grupe, D., et al. 2023b, *ApJ*, **944**, 177
- Komossa, S., Kraus, A., Grupe, D., et al. 2023c, *AN*, **344**, e20220126
- Komossa, S., Grupe, D., Marziani, P., et al. 2024, arXiv e-prints, (DOI: 10.48550/arXiv.2408.00089), arXiv:2408.00089
- Kovačević, A. B., Popović, L. Č., Simić, S., and Ilić, D. 2019, *ApJ*, **871**, 32
- Kovačević, A. B., Ilić, D., Popović, L. Č., et al. 2021, *MNRAS*, **505**, 5012
- Kovačević, A. B., Radović, V., Ilić, D., et al. 2022, *ApJS*, **262**, 49
- Laha, S., Meyer, E., Roychowdhury, A., et al. 2022, *ApJ*, **931**, 5
- Laine, S., Dey, L., Valtonen, M., et al. 2020, *ApJL*, **894**, L1
- LaMassa, S. M., Cales, S., Moran, E. C., et al. 2015, *ApJ*, **800**, 144
- Laor, A. and Brandt, W. N. 2002, *ApJ*, **569**, 641
- Lawrence, A. 2018, *NatAs*, **2**, 102
- Lawther, D., Vestergaard, M., Raimundo, S., et al. 2023, *MNRAS*, **519**, 3903
- Lehto, H. J. and Valtonen, M. J. 1996, *ApJ*, **460**, 207
- Leighly, K. M., Hamann, F., Casebeer, D. A. and Grupe, D. 2009, *ApJ*, **701**, 176
- Li, J., Sun, M., Wang, T., He, Z. and Xue, Y. 2019, *MNRAS*, **487**, 4592
- Lightman, A. P. and Eardley, D. M. 1974, *ApJL*, **187**, L1
- Liu, F. K. and Wu, X. B. 2002, *A&A*, **388**, L48
- Liu, F. K., Li, S. and Komossa, S. 2014, *ApJ*, **786**, 103
- Liu, H., Parker, M. L., Jiang, J., et al. 2021, *MNRAS*, **506**, 5190
- Liu, H.-Y., Liu, W.-J., Dong, X.-B., et al. 2019, *ApJS*, **243**, 21
- Liu, T., Gezari, S., Burgett, W., et al. 2016, *ApJ*, **833**, 6
- Longinotti, A. L., Kriss, G., Krongold, Y., et al. 2019, *ApJ*, **875**, 150
- Lynden-Bell, D. 1969, *Natur*, **223**, 690
- Lyutyj, V. M., Oknyanskij, V. L. and Chuvayev, K. K. 1984, *PAZh*, **10**, 803
- MacLeod, C. L., Ross, N. P., Lawrence, A., et al. 2016, *MNRAS*, **457**, 389
- MacLeod, C. L., Green, P. J., Anderson, S. F., et al. 2019, *ApJ*, **874**, 8
- MacLeod, M., Ramirez-Ruiz, E., Grady, S. and Guillochon, J. 2013, *ApJ*, **777**, 133
- Malyali, A., Liu, Z., Rau, A., et al. 2023, *MNRAS*, **520**, 3549
- Mandel, I. and Levin, Y. 2015, *ApJL*, **805**, L4
- Marin, F., Hutsemékers, D., Lioudakis, I., et al. 2023, *A&A*, **673**, A126
- Marziani, P., Dultzin, D., Sulentic, J. W., et al. 2018, *FRASS*, **5**, 6
- Matt, G., Guainazzi, M. and Maiolino, R. 2003, *MNRAS*, **342**, 422
- McElroy, R. E., Husemann, B., Croom, S. M., et al. 2016, *A&A*, **593**, L8
- Mehdipour, M., Kriss, G. A., Brenneman, L. W., et al. 2022, *ApJ*, **925**, 84
- Meyer, E. T., Laha, S., Shuvo, O. I., et al. 2024, arXiv e-prints, (DOI: 10.48550/arXiv.2406.18061), arXiv:2406.18061
- Mondal, S. and Stalin, C. S. 2021, *Galaxies*, **9**, 21
- Netzer, H. and Peterson, B. M. 1997, in *Astrophysics and Space Science Library*, Vol. 218, *Astronomical Time Series*, ed. D. Maoz, A. Sternberg and E. M. Leibowitz, 85
- Nicastro, F. 2000, *ApJL*, **530**, L65
- Noda, H. and Done, C. 2018, *MNRAS*, **480**, 3898
- Ochmann, M. W., Kollatschny, W. and Zetzl, M. 2020, *Contributions of the Astronomical Observatory Skalnaté Pleso*, **50**, 318
- Ochmann, M. W., Kollatschny, W., Probst, M. A., et al. 2024, *A&A*, **686**, A17
- Oh, K., Koss, M., Markwardt, C. B., et al. 2018, *ApJS*, **235**, 4
- Oknyansky, V. L., Malanchev, K. L. and Gaskell, C. M. 2018, in *Revisiting Narrow-Line Seyfert 1 Galaxies and their Place in the Universe*, 12
- Oknyansky, V. L., Winkler, H., Tsygankov, S. S., et al. 2019, *MNRAS*, **483**, 558
- Oknyansky, V. L., Brotherton, M. S., Tsygankov, S. S., et al. 2021, *MNRAS*, **505**, 1029
- Onken, C. A., Peterson, B. M., Dietrich, M., Robinson, A. and Salamanca, I. M. 2003, *ApJ*, **585**, 121
- Osterbrock, D. E. 1989, (Mill Valley, California: University Science Books)

- Pan, X., Lu, H., Komossa, S., et al. 2019, *ApJ*, **870**, 75
- Pan, X., Li, S.-L. and Cao, X. 2021, *ApJ*, **910**, 97
- Panda, S. and Śniegowska, M. 2024, *ApJS*, **272**, 13
- Parker, M. L., Komossa, S., Kollatschny, W., et al. 2016, *MNRAS*, **461**, 1927
- Parker, M. L., Longinotti, A. L., Schartel, N., et al. 2019a, *MNRAS*, **490**, 683
- Parker, M. L., Schartel, N., Grupe, D., et al. 2019b, *MNRAS*, **483**, L88
- Penston, M. V. and Perez, E. 1984, *MNRAS*, **211**, 33P
- Peterson, B. M. 1985, *IAU Circ.*, **4036**, 1
- Petrushevska, T., Leloudas, G., Ilić, D., et al. 2023, *A&A*, **669**, A140
- Popović, L. Č. 2012, *NewAR*, **56**, 74
- Popović, L. Č., Simić, S., Kovačević, A. and Ilić, D. 2021, *MNRAS*, **505**, 5192
- Popović, L. Č., Ilić, D., Burenkov, A., et al. 2023, *A&A*, **675**, A178
- Potts, B. and Villforth, C. 2021, *A&A*, **650**, A33
- Raj, A., Nixon, C. J. and Doğan, S. 2021, *ApJ*, **909**, 81
- Rees, M. J. 1990, *Sci*, **247**, 817
- Ren, G.-W., Ding, N., Zhang, X., et al. 2021, *MNRAS*, **506**, 3791
- Ricci, C., Kara, E., Loewenstein, M., et al. 2020, *ApJL*, **898**, L1
- Rodriguez, C., Taylor, G. B., Zavala, R. T., et al. 2006, *ApJ*, **646**, 49
- Roming, P. W. A., Kennedy, T. E., Mason, K. O., et al. 2005, *SSRv*, **120**, 95
- Ross, N. P., Ford, K. E. S., Graham, M., et al. 2018, *MNRAS*, **480**, 4468
- Ruan, J. J., Anderson, S. F., Cales, S. L., et al. 2016, *ApJ*, **826**, 188
- Runco, J. N., Cosens, M., Bennert, V. N., et al. 2016, *ApJ*, **821**, 33
- Runnoe, J. C., Eracleous, M., Pennell, A., et al. 2017, *MNRAS*, **468**, 1683
- Salpeter, E. E. 1964, *ApJ*, **140**, 796
- Savić, D., Marin, F. and Popović, L. Č. 2019, *A&A*, **623**, A56
- Savić, D., Hutsemékers, D. and Sluse, D. 2024, arXiv e-prints, (DOI: 10.48550/arXiv.2405.09303), arXiv:2405.09303
- Scepi, N., Begelman, M. C. and Dexter, J. 2021, *MNRAS*, **502**, L50
- Seyfert, C. K. 1943, *ApJ*, **97**, 28
- Shapovalova, A. I., Doroshenko, V. T., Bochkarev, N. G., et al. 2004, *A&A*, **422**, 925
- Shapovalova, A. I., Popović, L. Č., et al. 2019, *MNRAS*, **485**, 4790
- Shappee, B. J., Prieto, J. L., Grupe, D., et al. 2014, *ApJ*, **788**, 48
- Shen, Y. and Loeb, A. 2010, *ApJ*, **725**, 249
- Shen, Y., Liu, X., Loeb, A. and Tremaine, S. 2013, *ApJ*, **775**, 49
- Shobbrook, R. R. 1966, *MNRAS*, **131**, 293
- Sillanpaa, A., Haarala, S., Valtonen, M. J., Sundelius, B., and Byrd, G. G. 1988, *ApJ*, **325**, 628
- Simić, S., Popović, L. Č., Kovačević, A. and Ilić, D. 2022, *AN*, **343**, e210073
- Śniegowska, M., Czerny, B., Bon, E. and Bon, N. 2020, *A&A*, **641**, A167
- Stern, D., McKernan, B., Graham, M. J., et al. 2018, *ApJ*, **864**, 27
- Stone, N. C. and Metzger, B. D. 2016, *MNRAS*, **455**, 859
- Sulentic, J. W., Zwitter, T., Marziani, P. and Dultzin-Hacyan, D. 2000, *ApJL*, **536**, L5
- Syer, D., Clarke, C. J. and Rees, M. J. 1991, *MNRAS*, **250**, 505
- Tanaka, T. L. 2013, *MNRAS*, **434**, 2275
- Temple, M. J., Ricci, C., Koss, M. J., et al. 2023, *MNRAS*, **518**, 2938
- Terreran, G., Berton, M., Benetti, S., et al. 2016, *ATel*, **9417**, 1
- Tohline, J. E. and Osterbrock, D. E. 1976, *ApJL*, **210**, L117
- Trakhtenbrot, B., Arcavi, I., MacLeod, C. L., et al. 2019, *ApJ*, **883**, 94
- Truemper, J. 1982, *AdSpR*, **2**, 241
- Tsalmantza, P., Decarli, R., Dotti, M. and Hogg, D. W. 2011, *ApJ*, **738**, 20
- Ulrich, M.-H., Maraschi, L. and Urry, C. M. 1997, *ARA&A*, **35**, 445
- Urry, C. M. 1998, *AdSpR*, **21**, 89
- Valtaoja, E., Teräsanta, H., Tornikoski, M., et al. 2000, *ApJ*, **531**, 744
- Valtonen, M. J., Zola, S., Gopakumar, A., et al. 2022, arXiv e-prints, (DOI: 10.48550/arXiv.2209.08360), arXiv:2209.08360
- Vaughan, S., Uttley, P., Markowitz, A. G., et al. 2016, *MNRAS*, **461**, 3145
- Verbiest, J. P. W., Vigeland, S. J., Porayko, N. K., Chen, S. and Reardon, D. J. 2024, *ResPh*, **61**, 107719
- Véron-Cetty, M. P., Véron, P. and Gonçalves, A. C. 2001, *A&A*, **372**, 730
- Vestergaard, M. and Peterson, B. M. 2006, *ApJ*, **641**, 689
- Villata, M., Raiteri, C. M., Sillanpaa, A. and Takalo, L. O. 1998, *MNRAS*, **293**, L13
- Villforth, C., Nilsson, K., Heidt, J., et al. 2010, *MNRAS*, **402**, 2087
- Wanders, I., van Groningen, E., Alloin, D., et al. 1993, *A&A*, **269**, 39
- Wang, J., Xu, D. W. and Wei, J. Y. 2018, *ApJ*, **858**, 49
- Wang, J., Xu, D. W., Cao, X., et al. 2024a, *ApJ*, **970**, 85
- Wang, J.-M. and Bon, E. 2020, *A&A*, **643**, L9
- Wang, L., Greene, J. E., Ju, W., et al. 2017, *ApJ*, **834**, 129
- Wang, S., Woo, J.-H., Gallo, E., et al. 2024b, *ApJ*, **966**, 128
- Wei, J., Cordier, B., Antier, S., et al. 2016, arXiv e-prints, (DOI: 10.48550/arXiv.1610.06892), arXiv:1610.06892
- Wiseman, P., Wang, Y., Hönig, S., et al. 2023, *MNRAS*, **522**, 3992
- Wiseman, P., Williams, R. D., Arcavi, I., et al. 2024, arXiv e-prints, (DOI: 10.48550/arXiv.2406.11552), arXiv:2406.11552
- Wright, E. L. 2006, *PASP*, **118**, 1711
- Xin, C. and Haiman, Z. 2021, *MNRAS*, **506**, 2408

- Xin, C. and Haiman, Z. 2024, arXiv e-prints, (DOI: 10.48550/arXiv.2403.18751), arXiv:2403.18751
- Xu, D., Komossa, S., Zhou, H., Wang, T. and Wei, J. 2007, *ApJ*, **670**, 60
- Xu, D., Komossa, S., Zhou, H., et al. 2012, *AJ*, **143**, 83
- Xu, D. W., Komossa, S., Grupe, D., et al. 2024, *Univ*, **10**, 61
- Yang, J., van Bemmel, I., Paragi, Z., et al. 2021, *MNRAS*, **502**, L61
- Yang, Q., Wu, X.-B., Fan, X., et al. 2018, *ApJ*, **862**, 109
- Yardley, D. R. B., Hobbs, G. B., Jenet, F. A., et al. 2010, *MNRAS*, **407**, 669
- York, D. G., Adelman, J., Anderson, John E., J., et al. 2000, *AJ*, **120**, 1579
- Zelty, G., Trakhtenbrot, B., Eracleous, M., et al. 2024, *ApJ*, **966**, 85
- Zrake, J., Clyburn, M., and Feyan, S. 2024, arXiv e-prints, (DOI: 10.48550/arXiv.2410.04961), arXiv:2410.04961

ЕКСТРЕМИ ПРОМЕНЉИВОСТИ КОНТИНУУМА И ЕМИСИОНИХ ЛИНИЈА КОД АГЈ: ПРОМЕНЉИВА АКТИВНОСТ КОД АГЈ И ДВОЈНЕ СУПЕРМАСИВНЕ ЦРНЕ РУПЕ

S. Komossa¹  and D. Grupe² 

¹*Max-Planck-Institut für Radioastronomie, Auf dem Hügel 69, 53121 Bonn, Germany*

E-mail: skomossa@mpifr.de

²*Department of Physics, Geology, and Engineering Technology, Northern Kentucky University, 1 Nunn Drive, Highland Heights, KY 41099, USA*

УДК 524.882 : 524.7

Прегледни рад по позиву

Екстремни варијабилности емисионих линија и континуума код активних галактичких језгара (АГЈ) пружају јединствену могућност за тестирање физике и геометрије њихових централних извора енергије. Овај прегледни рад даје увид у најекстремније случајеве променљивости континуума и оптичких емисионих линија код АГЈ-а, као и објашњења ових ефеката. Такође указујемо на изазове у идентификацији АГЈ-а са променљивом активношћу ("променљивог изгледа", енг. "changing-look" – CL) и дискутујемо будуће правце истраживања у овој области. Указујемо на потребу за проналажењем већег броја CL АГЈа са уским линијама типа Сејферт 1, као и CL LINER-а, који се налазе на супротним крајевима режима акреције. У другом делу се разматрају докази о семи-периодичној променљивости

емисије широких линија и континуума, као и њихово могуће тумачење присуством двојних супермасивних црних рупа (енг. *Supermassive Black Holes* – SMBH). Представљени су најновији резултати пројекта МОМО, који интензивно прати најпознатијег кандидата за двојну супермасивну црну рупу, објекат ОЈ 287. Током последњих неколико година, резултати овог пројекта су одбацили постојећи модел двојног система и јасно указали на потребу за новим моделовањем овог двојног система у потпуно другачијем параметарском режиму, заснованом на стварно измереној маси (примарне) SMBH од $10^8 M_{\odot}$. Текући и будући прегледи неба који користе астрономију у временском домену, као и прва детекција гравитационих таласа из појединачних система, играће кључну улогу у развоју астрофизике.